

**EFFECT OF AMINO ACID SUBSTITUTIONS AT Asn 89 AND
Thr 148 OF CYT2Aa2 TOXIN FROM *Bacillus thuringiensis***

BOONSAN PRASERTKULCHAI

**A THESIS SUBMITTED IN PARTIAL FULFILLMENT
OF THE REQUIREMENTS FOR
THE DEGREE OF MASTER OF SCIENCE
(MOLECULAR GENETICS AND GENETIC ENGINEERING)
FACULTY OF GRADUATE STUDIES
MAHIDOL UNIVERSITY
2008**

COPYRIGHT OF MAHIDOL UNIVERSITY

Thesis
Entitled
**EFFECT OF AMINO ACID SUBSTITUTIONS AT Asn 89 AND
Thr 148 OF CYT2Aa2 TOXIN FROM *Bacillus thuringiensis***

.....
Mr. Boonsan Prasertkulchai
Candidate

.....
Assoc. Prof. Chartchai Krittanai, Ph.D.
Major-Advisor

.....
Asst. Prof. Boonhiang Promdonkoy,
Ph.D.
Co-Advisor

.....
Asst. Prof. Panadda Boonserm, Ph.D.
Co-Advisor

.....
Prof. Banchong Mahaisavariya, M.D.
Dean
Faculty of Graduate Studies

.....
Assoc. Prof. Varaporn Akkarapatumwong,
Ph.D.
Chair
Master of Science Programme in
Molecular Genetics and Genetic
Engineering
Institute of Molecular Biology and
Genetics

ACKNOWLEDGEMENTS

This thesis would not be accomplished if there are no valuable suggestions, extensive support and assistance from my major advisor, Assoc. Prof. Chartchai Krittanai and my co-advisers, Asst. Prof. Boonhiang Promdonkoy, Asst. Prof. Panadda Boonserm. I sincerely thank them for their valuable advice and guidance in this research.

I am very grateful to Miss. Anchanee Sangcharoen, Miss Somruathai Kidsanguan, Dr. Apichai Bourchookarn, Dr. Pattrara-Orn Chongsatja and Miss Wanwarang Pathaichindachote for suggestions, discussion including practice of laboratory techniques and Ms. Sukitaya Veeranondha for MTT assay. I would like to thank all of my friends for their encouragement and all staff of the Institute of Molecular Biology and Genetics who contribute in the success of my research project.

Finally, I would to thank my family from the deepest of my heart for their love and encouragement in study and project.

Boonsan Prasertkulchai

EFFECT OF AMINO ACID SUBSTITUTIONS AT Asn 89 AND Thr 148 OF
CYT2Aa2 TOXIN FROM *Bacillus thuringiensis*

BOONSAN PRASERTKULCHAI 4837269 MBMG/M

M.Sc. (MOLECULAR GENETICS AND GENETIC ENGINEERING)

THESIS ADVISORS: CHARTCHAI KRITTANAI, Ph.D.,
BOONHIANG PROMDONKOY, Ph.D., PANADDA BOONSERM, Ph.D.

ABSTRACT

The cytolytic toxin, Cyt2Aa2, is produced from *Bacillus thuringiensis* subsp. *darmstadiensis* during the sporulation stage. It is toxic to *dipteran* larvae *in vivo*, whilst it has a broad-range cytolytic activity *in vitro*. The N89K and T148K mutant toxins were constructed by site-directed mutagenesis, introducing positively charged residue into position 89 after α B and position 148 between α D and β 4. The results show that mutagenesis at residue Asn 89 does not affect the structural and functional activities of the toxin. Although mutagenesis on Thr 148 does not change the tertiary structure and larvicidal activity of Cyt2Aa2 toxin, it has an effect on structural stability. The T148K mutant shows a decrease in both solubility of the toxin in carbonate buffer and *in vitro* activities, i.e., oligomerization and hemolytic activity. The data suggest that Asn 89 is not a key residue involved in the structure and function of the toxin molecule. On the other hand, Thr 148 may take part in the membrane recognition of Cyt2Aa2. Moreover, the Lys substitution at residue 148 may interrupt the dimer formation of protoxin. These results demonstrate that the substitution of Thr with Lys at position 148 can help increase specificity of Cyt2Aa2, by maintaining *in vivo* activity and reducing *in vitro* toxicity. It provides improved knowledge of the cytolytic toxin with possible benefits for biotechnological applications.

KEY WORDS: *Bacillus thuringiensis* / LOOP α D AND β 4 / CYTOLYTIC
PROTEIN / CYT2Aa2/ LYSINE SUBSTITUTION /
/MOSQUITOCIDAL TOXIN

76 pp.

ผลกระทบของการเปลี่ยนแปลงกรดอะมิโนที่ตำแหน่งของ Asn 89 และ Thr 148 ของ โปรตีน Cyt2Aa2 จาก *Bacillus thuringiensis*
(EFFECT OF AMINO ACID SUBSTITUTIONS AT Asn 89 AND Thr 148 OF CYT2Aa2 TOXIN FROM *Bacillus thuringiensis*)

บุญสรרך ประเสริฐกุลชัย 4837269 MBMG/M

วท.ม. (อณุปันธุศาสตร์และพันธุวิศวกรรมศาสตร์)

คณะกรรมการควบคุมวิทยานิพนธ์ : ชาติชาย กฤตชัย, Ph.D. บุญเสียง พรหมดอนกอย, Ph.D.,
ปนัดดา บุญเสริม, Ph.D.

บทคัดย่อ

Cyt2Aa2 เป็นโปรตีนที่มีฤทธิ์ฆ่าลูกน้ำยุงซึ่งผลิตมาจาก *Bacillus thuringiensis* สายพันธุ์ *darmsadiensis* โปรตีนชนิดนี้มีจำเพาะต่อลูกน้ำยุงลายและทำให้เยื่อหุ้มของเซลล์หลายชนิดแตกได้ในหลอดทดลอง งานวิจัยนี้ได้ทำการศึกษาการแทนที่ของกรดอะมิโน Asn 89 และกรดอะมิโน Thr 148 ด้วยกรดอะมิโน Lys โดยวิธีก่อกลายพันธุ์ที่ตำแหน่งจำเพาะ ผลจากการวิเคราะห์คุณสมบัติต่างๆของโปรตีนกลายพันธุ์ทั้งสองพบว่าโปรตีนกลายพันธุ์ N89K และ T148K ยังคงมีความสามารถในการฆ่าลูกน้ำยุงเท่ากับโปรตีนต้นแบบ ในการทดสอบความสามารถในการรวมตัวกันของโปรตีนในเยื่อหุ้มเซลล์สังเคราะห์ และการทำให้มีคเล็ดแดงแตกในหลอดทดลองพบว่าโปรตีนกลายพันธุ์ N89K ไม่มีความแตกต่างจากโปรตีนดั้งเดิม ส่วนโปรตีนกลายพันธุ์ T148K มีความสามารถเหล่านี้ลดลงมาก และเมื่อทดสอบกับเซลล์เพาะเลี้ยงชนิดต่างๆพบว่าโปรตีนกลายพันธุ์นี้ได้สูญเสียความเป็นพิษต่อเซลล์เหล่านั้นด้วย ข้อมูลดังกล่าวแสดงให้เห็นว่ากรดอะมิโน Asn 89 มีได้มีบทบาทสำคัญในการรักษาโครงสร้างและเกี่ยวข้องกับการทำหน้าที่ของโปรตีน Cyt2Aa2 ในทางตรงกันข้ามกรดอะมิโน Thr 148 น่าจะมีบทบาทที่เกี่ยวข้องในการยึดเกาะของโปรตีนกับเยื่อหุ้มเซลล์ของสิ่งมีชีวิตอย่างจำเพาะ โดยความรู้ที่ได้นี้จะนำไปสู่การพัฒนาและปรับปรุงโปรตีน Cyt2Aa2 ให้มีความจำเพาะต่อเซลล์ของลูกน้ำยุงมากขึ้นและเป็นพิษต่อเซลล์อื่นๆน้อยลง อันจะเป็นประโยชน์ต่อการประยุกต์เพื่อใช้ในการควบคุมยุงพาหะของโรคต่อไปในอนาคต

CONTENTS

| | Page |
|--|-------------|
| ACKNOWLEDGEMENTS | iii |
| ABSTRACT | iv |
| LIST OF TABLES | ix |
| LIST OF FIGURES | x |
| LIST OF ABBREVIATION | xii |
| CHAPTER | |
| I. INTRODUCTION | 1 |
| 1.1 <i>Bacillus thuringiensis</i> | 1 |
| 1.2 Cytolytic toxins | 3 |
| 1.2.1 Genetics of cytolitic toxins | 3 |
| 1.2.2 Toxin structure and function | 4 |
| 1.2.3 The proposed mechanism of cytolitic toxins | 8 |
| 1.3 The benefits of cytolitic toxins | 16 |
| II. OBJECTIVES | 18 |
| III. MATERIALS | 19 |
| 3.1 Chemicals | 19 |
| 3.2 Bacteria strain | 19 |
| 3.3 Bacteria culture media | 19 |
| 3.4 Enzymes and Proteases | 21 |
| 3.4.1 Proteases | 21 |
| 3.4.2 Restriction endonucleases | 21 |
| 3.5 Oligonucleotide primers | 22 |
| 3.6 Miscellaneous | 22 |
| IV. METHODS | 24 |
| 4.1 DNA preparation using alkaline lysis | 24 |
| 4.2 Agarose gel electrophoresis | 25 |

CONTENT (CONT.)

| | Page |
|---|-------------|
| 4.3 Site-directed mutagenesis | 25 |
| 4.4 The template elimination by <i>DpnI</i> digestion | 28 |
| 4.5 Introduction of DNA plasmid into <i>E. coli</i> using heat-shock method | 28 |
| 4.6 Preparation of competent cells by $MgCl_2$ - $CaCl_2$ | 30 |
| 4.7 Screening for the mutated clones | 30 |
| 4.7.1 Mutant screening by restriction enzyme analysis | 30 |
| 4.7.2 Automated DNA sequencing analysis | 30 |
| 4.8 SDS-Polyacrylamide Gel Electrophoresis (SDS-PAGE) | 31 |
| 4.8.1 SDS-PAGE analysis using coomassie blue staining | 31 |
| 4.8.2 Silver staining of SDS-PAGE gel | 31 |
| 4.9 Protein concentration assay using Bradford reagent | 32 |
| 4.10 Western blot analysis | 32 |
| 4.11 Cytolytic protoxins preparation | 33 |
| 4.12 Protoxin solubilization and proteolytic processing | 34 |
| 4.13 Protein purification using Superdex™ 200 | 34 |
| 4.14 Protein concentration assay using UV-absorption spectroscopy | 34 |
| 4.15 Tertiary structure analysis using intrinsic fluorescence spectroscopy | 35 |
| 4.16 Larvicidal activity assay | 35 |
| 4.17 Hemolytic activity assay | 35 |
| 4.18 Hemoglobin release assay | 36 |
| 4.19 Oligomerization assay | 36 |
| 4.20 MTT cytotoxicity assay | 37 |
| V. RESULTS | 38 |
| 5.1 The construction of mutant toxins | 38 |
| 5.2 Protein production and solubility | 38 |
| 5.3 Proteolytic processing of mutant toxins | 43 |
| 5.4 Protein purification by size exclusion chromatography | 43 |

CONTENT (CONT.)

| | Page |
|---|-------------|
| 5.5 Intrinsic fluorescence spectroscopy | 50 |
| 5.6 Trypsin digestion | 50 |
| 5.7 Larvicidal activity | 50 |
| 5.8 Hemolytic activity | 50 |
| 5.9 Hemoglobin release activity | 55 |
| 5.10 Oligomerization of the mutants | 55 |
| 5.11 MTT cytotoxicity assay | 55 |
| VI. DISCUSSION | 60 |
| VII. SUMMARY | 68 |
| REFERENCES | 69 |
| BIOGRAPHY | 76 |

LIST OF TABLES

| Table | Page |
|--|-------------|
| 1. List of <i>cyt</i> genes from several <i>Bacillus thuringiensis</i> strains | 5 |
| 2. List of restriction endonucleases and their recognition sites | 21 |
| 3. Temperature cycling parameters for site-directed mutagenesis | 29 |
| 4. The mosquitocidal activity of N89K and T148K mutant | 53 |
| 5. Cytotoxicity against four different cell lines | 59 |

LIST OF FIGURES

| Figure | Page |
|---|-------------|
| 1. Electron micrograph of <i>Bacillus thuringiensis</i> subsp. <i>israelensis</i> | 2 |
| 2. Phylogenic tree of Cyt toxin family | 6 |
| 3. The amino acid sequence alignment of Cyt1A and Cyt2A toxin corresponding to their biochemical and mutagenesis data | 7 |
| 4. Secondary structure of the monomeric Cyt2A δ -endotoxin | 9 |
| 5. Schem of the Cyt2A conformation (top view) | 10 |
| 6. Ribbon representation of dimer of Cyt2A toxin | 11 |
| 7. Proposed cytolytic mechanisms of Cyt toxin | 14 |
| 8. Proposed lytic pore architecture | 15 |
| 9. Map of the plasmid pGEM-T _{easy} containing <i>cyt2Aa2</i> gene | 20 |
| 10. Overview of QuikChange™ site-directed mutagenesis method (Stratagene) | 26 |
| 11. Position of Asn 89 and Thr 148 on the three dimensional structure of Cyt2Aa2 toxin | 27 |
| 12. Amplification of N89K and T148K mutant plasmids | 39 |
| 13. Restriction enzyme analysis and DNA sequencing of N89K mutant | 40 |
| 14. Restriction enzyme analysis and DNA sequencing of T148K mutant | 41 |
| 15. The protein expression of N89K and T148K mutant | 42 |
| 16. 12.5% SDS-PAGE gel of Cyt2Aa2, N89K and T148K mutants compared with their washing solution | 44 |
| 17. Western blot analysis of Cyt2Aa2, N89K and T148K protoxin | 45 |
| 18. The protein expression and solubility of the mutant toxins | 46 |
| 19. Proteolysis profile of proteinase K and chymotrypsin digestion | 47 |
| 20. Chromatographic profile for the purification of activated Cyt2Aa2 (A), N89K (B) and T148K mutant (C) | 48 |
| 21. 12.5% SDS-PAGE of the elution fraction from size-exclusion chromatography | 49 |

LIST OF FIGURES (CONT.)

| Figure | Page |
|---|-------------|
| 22. Intrinsic fluorescence spectra of the toxins | 51 |
| 23. Trypsin digestion profile of N89K and T148K on 15% SDS-PAGE gel (A) and Western blotting (B) | 52 |
| 24. Hemolytic activity | 54 |
| 25. Hemoglobin release activity of Cyt2Aa2, N89K and T148K | 56 |
| 26. Oligomerization analysis with coomassie blue staining | 57 |
| 27. Oligomerization detected with silver staining | 58 |
| 28. Possible conformation of lysine 89 that protect toxins from trypsin digestion | 63 |
| 29. Possible interaction of lysine 148 on the Cyt2Aa2 | 64 |

LIST OF ABBREVIATIONS

| | |
|----------------|---|
| % (w/w) | percent weight by weight |
| % C | percent of crosslink |
| % T | percent of gel |
| Amp | Ampicillin |
| ANS | 8-anilinonaphthalene-1-sulfonic acid |
| a.u. | arbitrary unit |
| BSA | bovine serum albumin |
| bp | basepairs |
| °C | degree Celsius |
| Cry | crystal |
| Cyt | cytolytic |
| DNA | Deoxyribonucleic acid |
| DTT | 1,4-dithiothreitol |
| <i>E. coli</i> | <i>Eschericia coli</i> |
| EDTA | ethylenediamine tetraamino acid |
| <i>et al.</i> | and others |
| EtBr | ethidium bromide |
| g | gram(s) |
| hr | hour(s) |
| IPTG | isopropyl- β -D-thiogalactopyranoside |
| kb | kilobase(s) |
| kDa | kilodalton(s) |
| LB | Luria-Bertani medium |
| M | molar (mol/l) |
| mg | milligram(s) |
| min | minute(s) |

LIST OF ABBREVIATIONS (CONT.)

| | |
|-------------------|---------------------------|
| ml | milliliter(s) |
| mM | millimolar |
| MW | molecular weight |
| μg | microgram(s) |
| ng | nanogram(s) |
| nm | nanometer(s) |
| N-terminal | amino terminal |
| C-terminal | carboxyl terminal |
| OD ₆₀₀ | optical density at 600 nm |
| OD ₅₉₅ | optical density at 595 nm |
| OD ₅₄₀ | optical density at 540 nm |
| psi | pound per square inch |
| RNA | ribonucleic acid |
| RNase A | ribonuclease A |
| rpm | revolution per minute |
| UV | ultraviolet |

CHAPTER I

INTRODUCTION

1.1 *Bacillus thuringiensis*

Bacillus thuringiensis is a Gram-positive, spore-forming soil bacterium. During the sporulation, *Bacillus thuringiensis* produces parasporal crystal proteins (1), as shown in **figure 1**, which are toxic to many species of insect larvae. These crystalline proteins are toxic against larvae belonging to the order of *Lepidoptera* (moths and butterflies), *Blattodea* (cockroaches), *Coleoptera* (beetles), *Diptera* (flies and mosquitoes) and *Hymenoptera* (bees and wasps) (2-5). In addition, the parasporal proteins have also been reported to be lethal to nematodes and protozoa (6). Based on their properties, these toxins were applied for a control of the serious disease vector (7-9), such as mosquitoes and black flies, and for agricultural pest, i.e., beetles and moths (10).

The previous reports revealed that a *B. thuringiensis* produces many kinds of crystal protoxins depending on the strains which are different in shape, size, biological property and activity (11-13). For example, *B. thuringiensis* var. *israelensis* is used in the field for a control of mosquito and blackflies (7-9), which are a vector of serious diseases, like dengue fever and river blindness diseases. *B. thuringiensis* subsp. *berliner* is a commercially available bacterial product for pest insect controlling of field crops (10). The mechanism of action of crystalline toxins are composed of 1) the solubilization of crystalline protoxin in the larval midgut, 2) the processing of toxin by midgut proteases, and 3) binding to the midgut-epithelium cell membrane and forming of the lytic pore. Firstly, the protoxin has to be ingested by the susceptible insect larvae. The protoxin is solubilized under the alkaline condition of the insect midgut, and then the protoxin is processed by many midgut proteases to be converted into active form (6, 14-16). Next, the active toxin recognizes to specific receptor or epithelial cell surface. After that the activated toxins insert into the

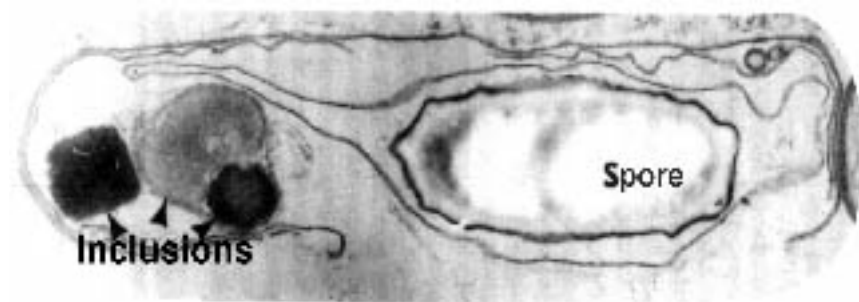


Figure 1: Electron micrograph of *Bacillus thuringiensis* subsp. *israelensis*.

The transmission electron micrograph shows the parasporal inclusion proteins of *Bacillus thuringiensis* subsp. *israelensis* during sporulation stage. The black arrow heads point the parasporal inclusion bodies (18).

membrane and form the lytic pore causing imbalance osmotic pressure, cell swelling and leading to cell lysis (6, 17).

1.2 Cytolytic toxins

Cytolytic toxins are δ -endotoxins produced by *Bacillus thuringiensis*. Among the δ -endotoxins were categorized as crystalline toxin (Cry toxins) and cytolitic toxin (Cyt toxins) (19). There are many differences between Cyt toxins and Cry toxins, for example, size, structure and host specificity. In general the molecular weight of cytolitic toxins (25-28 kDa) are smaller than that of crystalline toxins (20). The molecule of crystalline toxins could be determined to have three domains corresponding to different function, such as receptor binding domain and pore-forming domain (6). Cyt toxins are single domain composed of six α -helices and seven β -sheets (19). Cry toxins are toxic to *Lepidopteran*, *Dipteran* and *Coleopteran* larvae whereas Cyt toxins have toxicity against *Dipteran* larvae (20). Moreover, Cyt toxins are cytolitic to a broad range of cells *in vitro*, such as mosquito cells, mammalian cells and erythrocytes (21, 22).

1.2.1 Genetics of cytolitic toxins

In 1984, Ward, *et al.* could clone and transform the *cytA* gene of *B. thuringiensis* subsp. *israelensis* into *Escherichia coli* JM 101. The *cytA* gene (1,408 base-pairs) was analyzed and demonstrated all along the open reading frame encoding 27.34 kDa δ -endotoxin protein (23-25). The transcription start point is at 44 nucleotides upstream of initiation codon and a Shine-Dalgarno sequence located on 10 base-pair upstream of the start codon. At 3' end of this gene, an inverted repeat (IR) element forming stem-and-loop structure was found immediately after stop codon. The IR element has been proposed to act as a translational terminator (23, 24). In 1993, DNA fragment of the *cytB* gene (1,244 base-pairs) from *B. thuringiensis* subsp. *kyushuensis* was cloned into *E. coli* and the nucleotide sequence and protein expression levels were characterized (20). It is found to encode for the 29.2 kDa of CytB δ -endotoxin. A Shine-Dalgarno sequence is eight base-pair upstream of start codon. The *cytB* gene also has terminator secondary structure, which is nine base-pair hairpin loop and six base-pair stem loop, at position 1048-1086 downstream of

structural gene. The entire sequence has very low GC content of 27.1%. However the GC content of the structural itself is 28.5% (20). Nowadays, the novel cytolytic toxin genes have been cloned and isolated from many strains of *B. thuringiensis*. To organize the pool of data, a nomenclatural standard has been developed by genomic sequencing efforts. The closely related toxins, according to evolutionary divergence, have been ranked together (26). CytA becomes Cyt1A and CytB becomes Cyt2A. The list of cytolytic toxins and their strain of *B. thuringiensis* are shown in **table 1**. The phylogenetic tree of cytolytic toxins is shown in **figure 2** (27).

1.2.2 Toxin structure and function

Two well-known δ -endotoxins, Cyt1A and Cyt2A, are produced by *B. thuringiensis* subsp. *israelensis* and *kyushuensis*, respectively. In the early period of cytolytic toxins study, *Bacillus thuringiensis* subsp. *israelensis* has been reported to produce at least three δ -endotoxins, at molecular weight of 28, 68 and 130 kDa (28). These components were recognized by the immunological difference among each other but only the 28-kDa Cyt1A protein can demonstrated the haemolytic activity (28). Although, Cyt1A encoding gene is cloned and expressed as inclusion bodies in *E. coli* cells, it must require a 20 kDa helper-protein for co-expression (29). Some recent report has been proposed that the helper-protein improves *cyt* gene expression in *E. coli* cells through post-transcriptional regulation of the *cytA* gene (30). In contrast other publications suggested that the helper-protein affect neither post-transcription nor translational initiation (29). The function of this protein may bind on and prevent degradation of the nascent CytA polypeptide (31). On the other hand, 29 kDa Cyt2A δ -endotoxin could be cloned and expressed very well in the *E. coli* system without 20 kDa helper-protein (20).

In comparison the Cyt1A and Cyt2A endotoxin are composed of 249 (27.4 kDa) and 259 (29.2 kDa) amino acids, respectively (20, 23). The secondary structure of Cyt1A δ -endotoxin is similar to that of Cyt2A toxin. The alignment of amino acid sequences of these two proteins (**figure 3**) demonstrated a 39% identity and 70% similarity. The proteases cleavage sites of Cyt1A and Cyt2A are found at matching positions on the sequence alignment (32). In 1996, Jade Li *et al.* have determined the crystal structure of unprocessed Cyt2A by multiple isomorphous replacement (MIR)

Table 1: List of *cyt* genes from several *Bacillus thuringiensis* strains (33).

| Gene | Subspecies | Access No. [Reference] |
|----------------|---|-----------------------------------|
| <i>cyt1Aa1</i> | <i>israelensis</i> | X03182 (23) |
| <i>cyt1Aa2</i> | <i>israelensis</i> | X04338 (24) |
| <i>cyt1Aa3</i> | <i>morrisoni</i> PG14 | Y00135 (34) |
| <i>cyt1Aa4</i> | <i>morrisoni</i> PG14 | M35968 (35) |
| <i>cyt1Ab1</i> | <i>medellin</i> | X98793 (36) |
| <i>cyt1Ba1</i> | <i>neoleonensis</i> | U37196 (37) |
| <i>cyt2Aa1</i> | <i>kyushuensis</i> | Z14147 (20) |
| <i>cyt2Aa2</i> | <i>darmstadiensis</i> | AF472606 (38) |
| <i>cyt2Ba1</i> | <i>israelensis</i> | U52043 (39) |
| <i>cyt2Ba2</i> | <i>morrisoni</i> PG14 | AF020789(19) |
| <i>cyt2Ba3</i> | <i>fukuokaensis</i> | AF022884(19) |
| <i>cyt2Ba4</i> | <i>morrisoni</i> HD12 | AF022885(19) |
| <i>cyt2Ba5</i> | <i>morrisoni</i> HD518 | AF022886(19) |
| <i>cyt2Ba6</i> | <i>morrisoni</i> serovar <i>tenebrionis</i> | AF034926(19) |
| <i>cyt2Ba7</i> | strain T301 | AF215645 (40) |
| <i>cyt2Bb1</i> | <i>jegathesan</i> | U82519 (41) |
| <i>cyt2Bc1</i> | <i>medellin</i> | AJ251979 (42) |

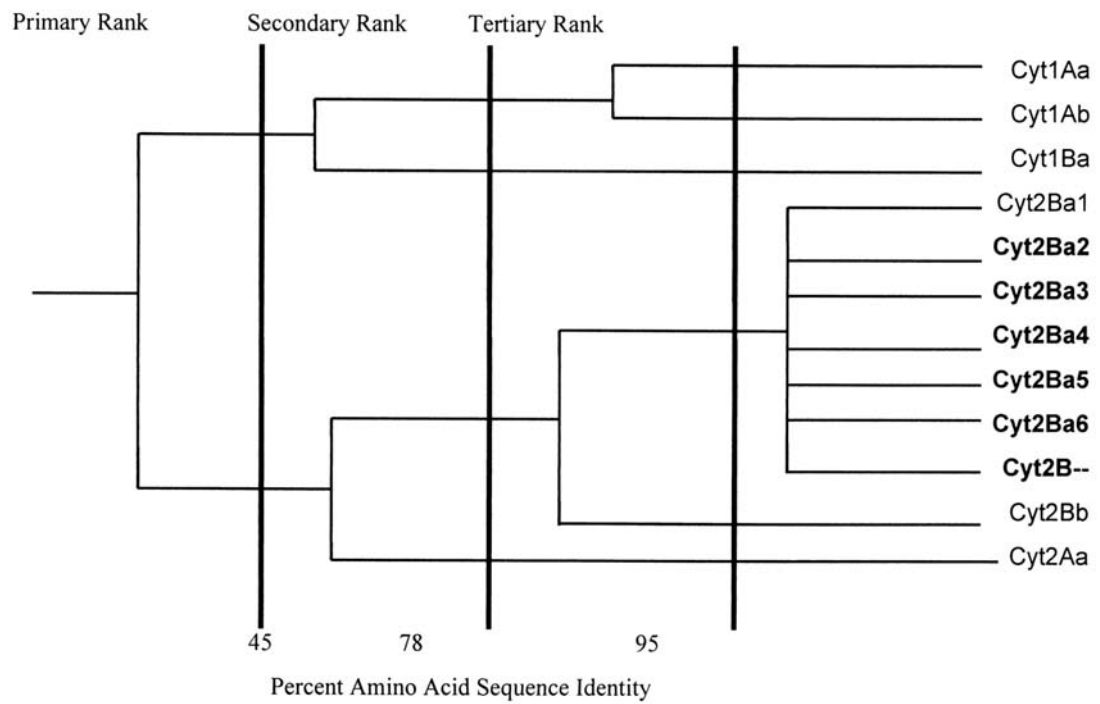


Figure 2: Phylogenetic tree of Cyt toxin family.

The figure illustrates the relationship between each cytolytic toxin gene. The dendrogram was constructed using National Center for Biotechnology Information's (NCBI) BLAST WWW server and the MegAlign program (27).

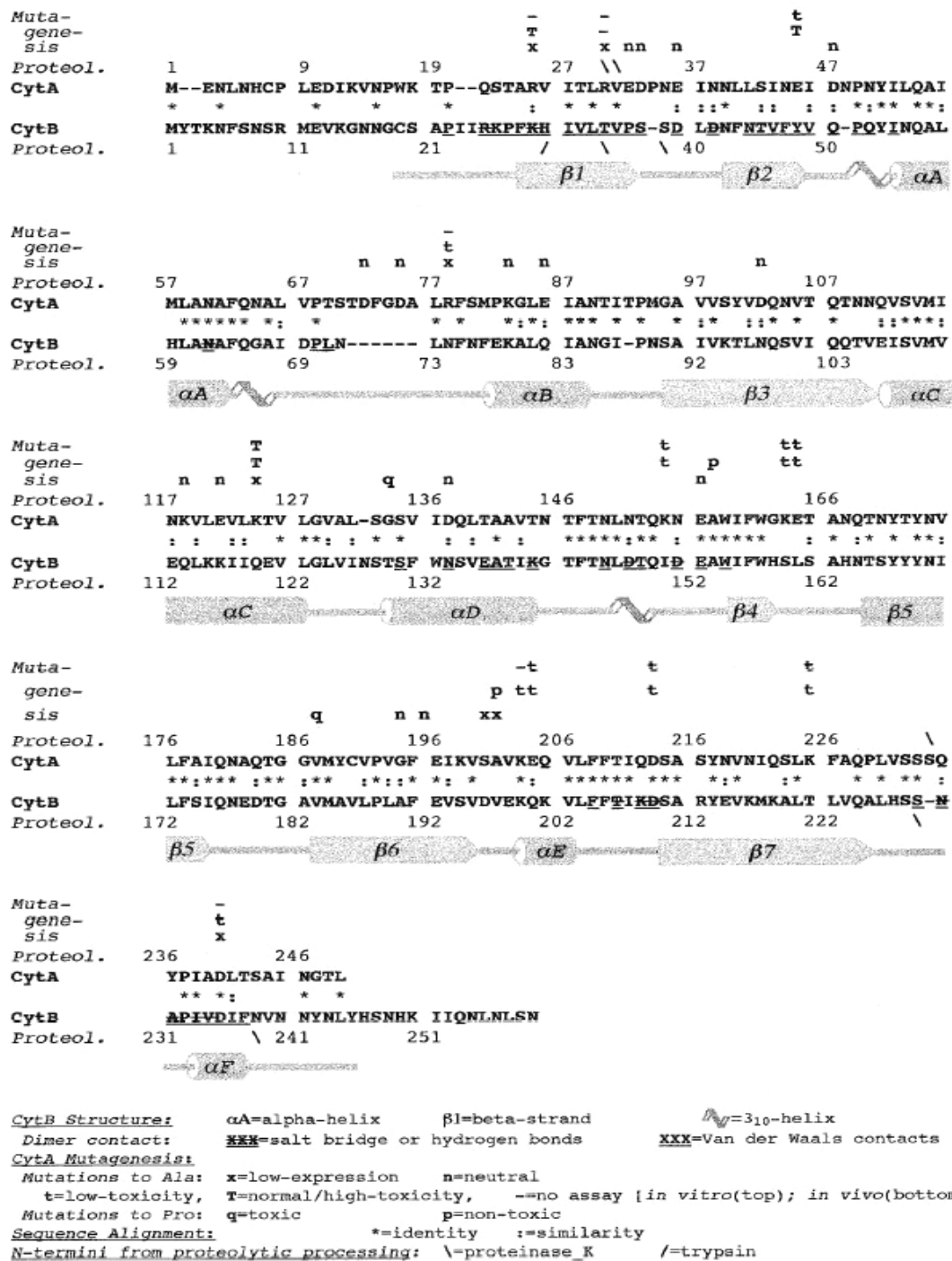


Figure 3: The amino acid sequence alignment of Cyt1A and Cyt2A toxin corresponding to their biochemical and mutagenesis data (19).

and X-ray data(19). Their work revealed that the structure of Cyt2A contains a single domain of α/β architecture, comprising of six α -helices and seven β -sheets (19) as shown in **figure 4**.

The toxin molecule has three layers, which are two outer layers of α -helix hairpins wrapped around a mixed β -sheet in the middle as shown in **figure 5**. The 55 residues or 24% of the toxin are six α -helices and the 75 residues or 33% of the polypeptide involving the β -sheet structure. There are three 3_{10} helices at N- and C-termini of α -helices A and in the loop connecting between α -helices D and β -strands 4. The α -helices have the amphipathic property, the hydrophobic residues face against the β -sheet while the polar and charge residues point out to the environment. The β -strands have shown strongly left-handed twist and amphipathic character in some of the β -sheets. The N-terminal part of protoxin Cyt2A is involved with dimerization between two molecules by intertwining with another N-terminal end from a further molecule (19). The protoxin dimers (**figure 6**) have been produced to stabilize secondary structure of the protoxin molecules. Moreover, the dimerization of Cyt2A toxin is involved with the other interactions presenting in five regions on the surface of each monomeric toxin (19). Firstly, the hydrogen bonds form $\beta 1'$ monomer (residue F28 to P36) to $\beta 1$ and $\beta 2$ of another monomer (residue N44 to Y48), in the opposite way, $\beta 1$ also forms the hydrogen bonds with $\beta 1'$ and $\beta 2'$. Secondly, the extended N-terminal part can form salt bridge and van der Waals interaction of with loop $_{\alpha D, \beta 4}$, loop $_{\beta 1, \beta 2}$, loop $_{\alpha A, \alpha B}$ of other monomer. Third area is between loop $_{\beta 7, \alpha F}$ and α helix F, Asn230 in loop $_{\beta 7, \alpha F}$ and Val234 in helix F form the hydrogen bonds with each other similar to Ala231 in loop $_{\beta 7, \alpha F}$ and Ile233 in helix F. The forth part is between helix D and loop $_{\alpha D, \beta 4}$ which are salt bridged between Lys140 and Asp147. The last region is loop $_{\alpha E, \beta 7}$ that form the salt bridge to each other (19). In addition, Cyt2A toxin has an extra 15 residue at C-terminal sequence that make a difference from Cyt1A (20). The additional amino acids of Cyt2A have been suggested to be proteolysis preventing residues.

1.2.3 The proposed mechanism of cytolytic toxins

In vivo, the cytolytic toxins have been identified to have a very specific toxicity against *Dipteran* larvae, i.e., mosquitoes and black flies(20). However, *in vitro*, the

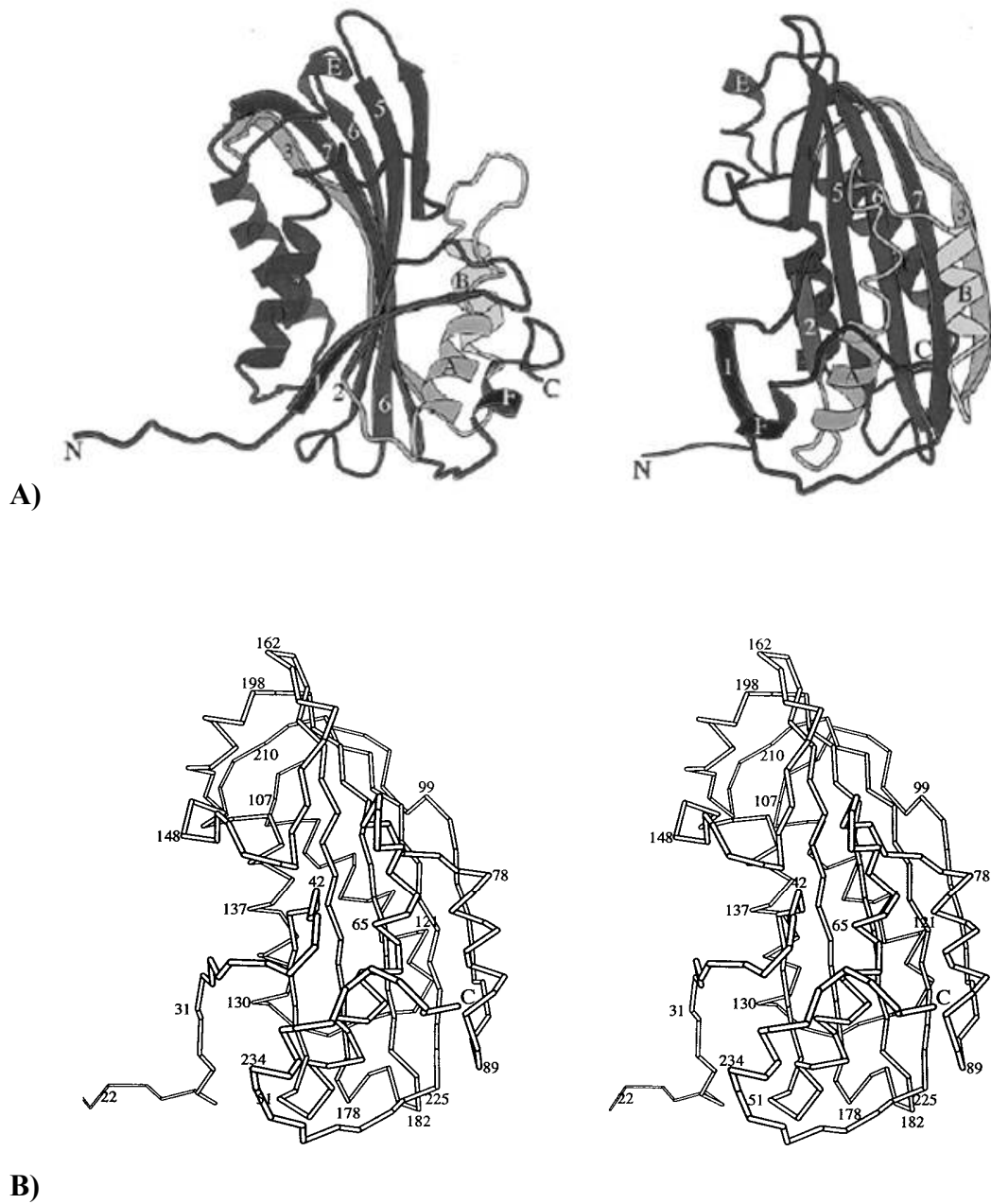


Figure 4: Secondary structure of the monomeric Cyt2A δ -endotoxin (19).

A) the ribbon model of a Cyt2A toxin, the side view of the toxin molecule shows the three layers of left-handed twisted β -sheets and two wrapped α -helices (as shown on the left) and the front view is showed on the right. B) the stereogram of the Cyt2A shows the face view of C^α trace of a toxin molecule.

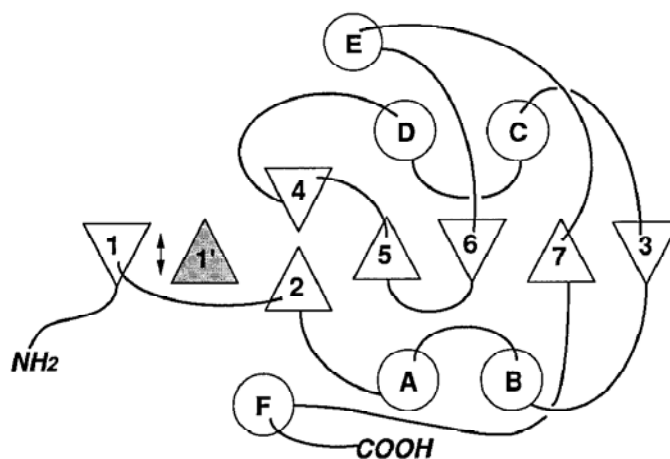


Figure 5: Scheme of the Cyt2A conformation (top view) (19).

The topology scheme shows conformation of the Cyt2A toxin. The circles with English alphabet are corresponded to the α -helices. The β -sheets are represented by the triangles. The direction of triangles is depended on the direction of the β -sheets, i.e., pointed down triangle represented pointed down β -strands.

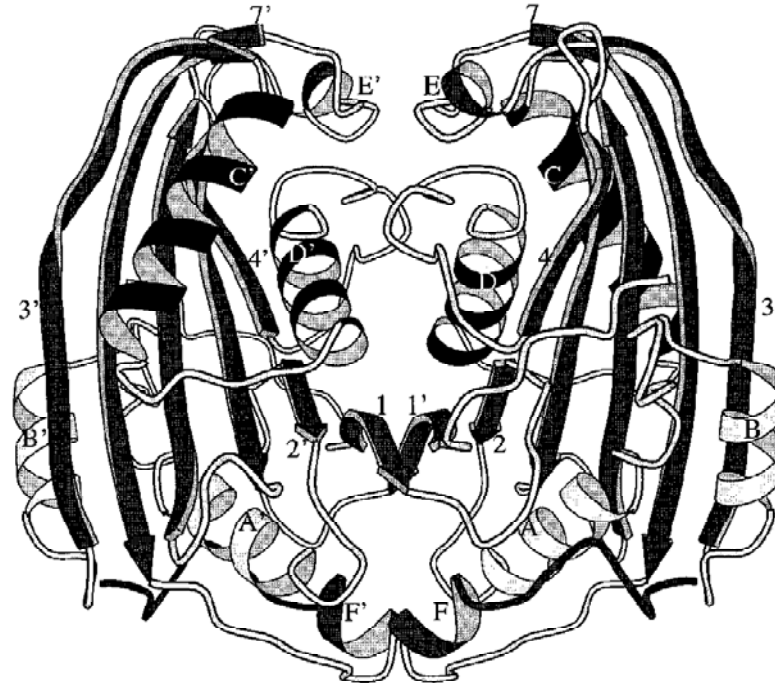


Figure 6: Ribbon representation of dimer of Cyt2A toxin.

The figure show dimeric form of Cyt2A protoxins. Two monomeric toxins are associated together by intertwining their N-terminal end and interaction between five points as previously described (19).

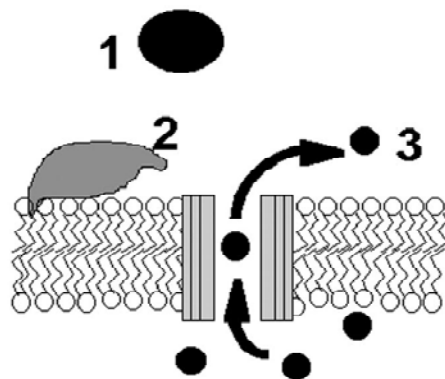
toxins show a broad-range spectrum of cytolytic activity (21, 22). For hemolytic activity assay Cyt1A toxin can lyse red blood cells, although it is not activated by any proteases. Unlike Cyt1A, Cyt2A endotoxin has to be activated by proteases, before its hemolytic activity is active (20). The different properties between Cyt1A and Cyt2A can be related to the additional 15 residue C-terminal sequence of Cyt2A toxin. In addition, the hemolytic activity of Cyt1A toxin may be due to the total charge on the surface of toxin molecule (20). A comparison of hydropathy plot of Cyt1A and Cyt2A illustrates a close property in high hydrophobicity especially in the C-terminus region. Their hydrophobicity are relatively increased after proteolysis (20). When Cyt1A protoxin is in the neutral pH, the net charge is about -7. After digested with trypsin, net charge of Cyt1A does not change significantly. The net charge removal the N-terminal or both termini of Cyt1A by proteinase K, give the negative net charge similar to that of processed Cyt1A (about -5 or -7, respectively). Whereas unprocessed Cyt2A has no net charge at the neutral condition (20).

The cytolytic mechanism of the toxin is occurred from ingestion of the toxin inclusion by insect larvae. Then, Cyt toxins are moved through digestive track and solubilized under alkaline condition of the larval midgut. The solubilized toxins are processed by gut proteases and become an active form.

In vivo, the processing of protease cleavage is still unknown. But the processing sites of proteinase K and trypsin *in vitro* have been determined. Proteinase K digests the Cyt2A toxin into 23 kDa fragments from Thr34 to Phe237. Furthermore overdigestion can also yield the 20 kDa fragment (Ser38 to Ser228). Both products are cytolytically active (32). Because the intertwined N-terminal fragment and β 1 sheet involved with dimerization were removed, the toxin will be released as monomer (19). The C-terminal arm and α F of the toxin were removed as well to show β layers core. Trypsin also digests the Cyt toxin but the resulting product is not active. Because trypsin just cleaves at His30 that is very close to the N-terminus of β 1 of Cyt2A. Hence, trypsin has failed to express the β -core of this toxin since it cannot eliminate the β 1 involving the dimerisation, thus the trypsin digested Cyt2A toxin will be in the dimer and inactive form. On the other hand, Cyt1A requires both of proteinase K and trypsin to dissociate the toxin to monomer by removal β 1 fragment from the molecule. After proteolysis, toxin molecule will separate to monomer

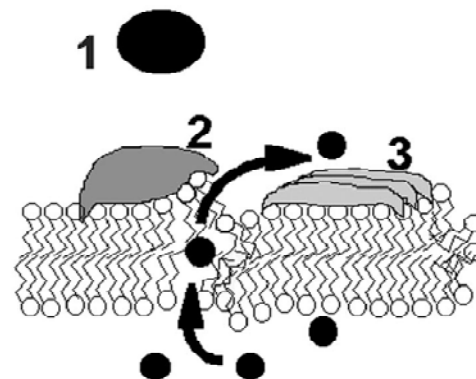
molecule and elucidate some hydrophobic residues. The conformational change does not occur during this stage. Next, the activated toxin will attach to the membrane (32). There are some reports proposed that the cytolytic toxin does not require specific receptors for binding but they could bind to all regions of larval midgut membrane. However, a similar case of receptor mediation has been reported in Cry toxin. It binds to specific receptors on the apical brush boarder of the midgut microvillae of susceptible insects with two-stage process of reversible and irreversible steps (6). While *in vivo* Cyt2A toxin apparently undergoes self-association after binding to the membrane.

In the step of toxin insertion, the two proposed mechanisms for cytolytic toxin are lytic pore forming model (19) and detergent-like model (43, 44) (**figure 7**). For the pore forming model, after binding to the membrane the conformation of this toxin starts to change by spreading the α -helices C and D out. Then the β -sheet 5, 6, and 7 are inserted into the membrane. The α -helices A and B are then inserted into membrane as well. After that, the membrane-bound toxins will aggregate with adjacent molecules and form the oligomeric lytic pore. The channel opening of cytolytic pore is reduced in the presence of divalent cations and the effect is reversed when these ions are removed. These data support a colloid-osmotic lysis mechanism. The study of Knowles et al (45) shows that Cyt1A can form the cation-selective channels in planar lipid bilayers. The experiment of Szabo *et al* (46) has demonstrated that synthetic peptide corresponding to helix C involves in toxic activity. In addition, Gazit & Shai (47) have synthesized and characterized two helices corresponding to helix A and C. The results have supported a role of two helices in the self-assembly and pore-formation. When the structure of Cyt2A was determined by Li J. *et al*, 1996 (19), the trans-membrane pore is proposed to be created by an aggregation of β -sheet 5, 6, and 7 (**figure 8**) similar to the β -barrel pore as the porin (48) and aerolysin toxin (49). These β -sheets are long enough to span the hydrophobic region of the bilayers-lipid membrane. Whereas α -helices A and B are expected to open out as the umbrella and lay on the membrane surface. The β -sheets are coiled with the α -helices A and B to demonstrate as the interior face of a β -barrel. Up to present, there are no direct evident that identify the number of toxin molecules that form the trans-membrane pore. Knowles & Ellar (1987) have proposed that if the lytic



THE PORE-FORMING MODEL

The protein **inserts** in the lipid bilayer.
 The protein has a specific **structure**.
 Pores are well-defined - **protein-lined**.
 Lipids are **well organized**.
 Membranes are **still there**, although leaky.



THE DETERGENT MODEL

The protein **does not** insert in the lipid bilayer.
 The protein may be **unstructured**.
 Pores are temporary, if any - **packing faults**.
 Lipids are **more disordered**.
 Membranes **break up** into protein/lipid complexes.

Figure 7: Proposed cytolytic mechanisms of Cyt toxin (43).

1) represents an active toxin, 2) the active toxin binds to phospholipid bilayer, 3) for pore forming model, the toxin molecules insert into the membrane and form the transmembrane pore. The detergent-like model, 3) the unsystematic aggregation of the toxins on the lipid membrane leads to the membrane crack.

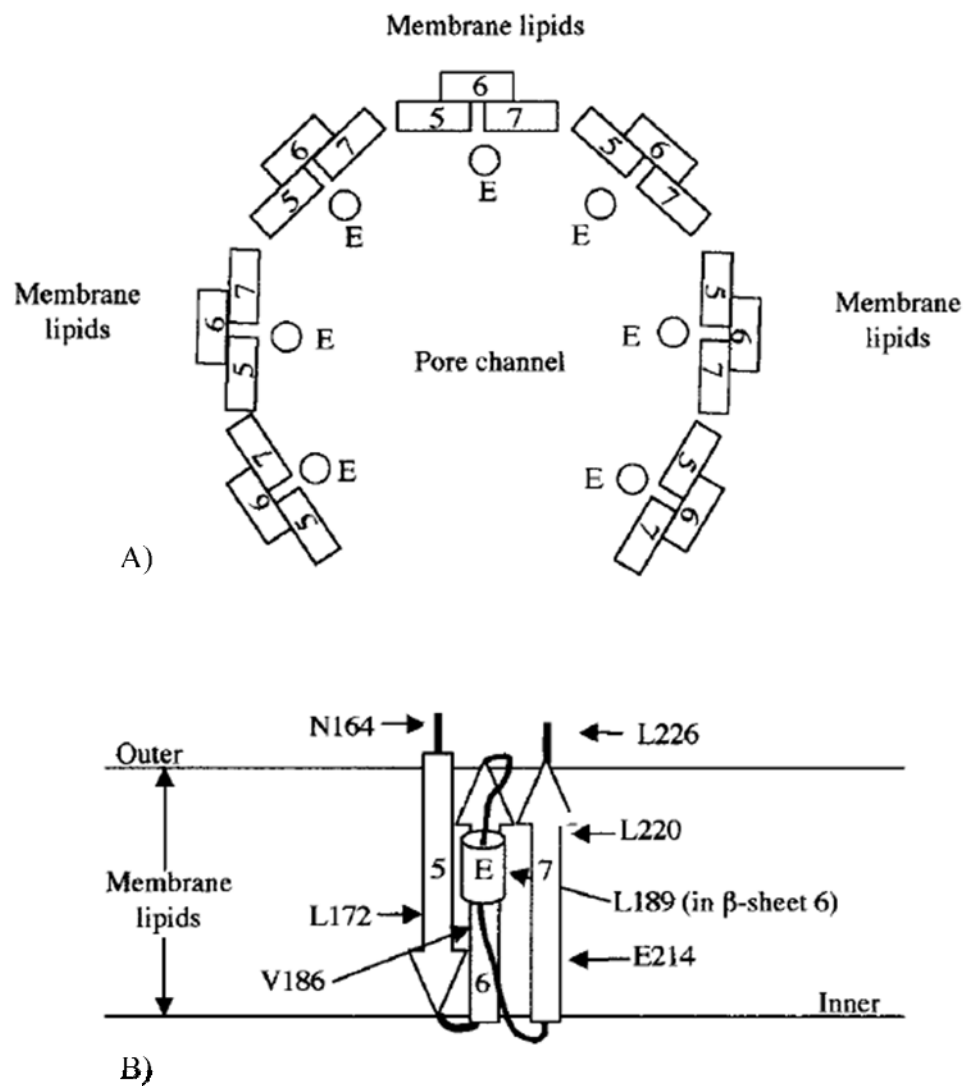


Figure 8: Proposed lytic pore architecture (50).

A) The top view of the lytic pore of Cyt2Aa1 endotoxin that have been predicted that the transmembrane pore was formed by arrangement of the β 5, β 6 and β 7 to form the β -barrel structure, B) the monomeric Cyt2Aa1 toxin and the membrane inserted residues predicted by site-directed mutagenesis.

pore is 5-10 nm in diameter (51), the number of monomer in the lytic pore should be about 4 or 6 monomers based on the prediction from the pore size of similar β -barrel toxin.

In contrast, Butko (43) has proposed another model, based on the detergent-like behavior of toxin. He did not agree with the cation-selective channels model because the lacking of direct evident to confirm (i) the number of the toxin molecule that used to form a lytic-pore, (ii) the limitation of size of the leakage from vesicle that lysed by Cyt1A, (iii) significant part of Cyt1A inserting in the lipid bilayer core. Thus, he proposed that the cytolytic toxin does not form the lytic pore but it break the membrane by aggregation between toxin molecules in the detergent-like manner (as shown in a **figure 7**). He suggested the experiments to prove the model i.e., ability for releasing large molecule (>100 kDa) from bilayers-lipid vesicle. If lytic pore (1-2 nm in diameter) were formed on the lipid membrane, the very large molecules should not be released from the vesicle. Moreover if the toxin forms the cation-selective channels on the membrane, size of the vesicle after releasing should not be changed. In 2005, Manceva reported the evidence that supports the detergent-like manner of Cyt toxin (44). His work included: (i) the analysis of lipid-toxin complex on SDS-PAGE, (ii) Fluorescence photobleaching recovery, and (iii) epifluorescence microscopy. These approaches provided information that the Cyt toxins aggregate into a broad-range of molecular weight and break the lipid vesicle into small particle (44). SDS-PAGE has shown a laddering pattern of various molecular weights rather than the band of hexamer of Cyt1A (~ 144 kDa). These results suggest that the Cyt1A toxins act in a detergent-like manner rather than forming the lytic pore on the cell membrane.

1.3 The benefits of Cytolytic toxins

The toxins produced from *Bacillus thuringiensis* have been applied for pest-controlling for many years instead of chemical insecticides, because the chemical insecticides have broad toxicity for organisms and can persist in the environment. The δ -endotoxin encoding gene from *Bacillus thuringiensis* has been transformed into the genome of many crops by DNA technology to construct the insect-resistance transgenic plants such as transgenic corns, tobaccos, tomatoes and, potatoes (52-54). Moreover, the δ -endotoxins from *Bacillus thuringiensis* and *Bacillus sphaericus* have

been used to control the serious disease vectors in the order *Diptera*, such as mosquitoes and blackflies or *Lepidoptera* order i.e., moths, and butterflies (55). Despite these transgenic organism and toxins give the promised result, they have been resulted in the production of resistance insect in moderate and high level, such as the *culex* mosquitoes resistant to Cry4A, Cry4B, Cry11Aa, and Bin toxins from *Bacillus sphaericus* (56). In the past few years, the problems of resistant mosquitoes have been solved by using synergism between two toxins or more (57). For example, Cry4Ba, in general, is not toxic to *C. quinquefasciatus* larvae (58). But the lethal activity of Cry4Ba δ -endotoxin against to *culex* larvae can be promoted by combination with Cyt2Aa2. Furthermore, cytolytic toxins, for example; Cyt1A and Cyt2Aa2, can also synergize with Cry11Aa, Cry4Aa, or Cry4Ba.

Nowadays, as the cytolytic toxins have a potential activity in cytopathogenic toxicity, there are attempts to use these toxins for killing cancer cells. However, for the medical applications, the toxins need to be improved for their specificity to the cancer cells by conjugation with antibodies or small protein fragment. Al-Yahyaee and co-workers, (1996) (59) have investigated the conjugation of CytA toxins with two monoclonal antibodies (mAb) against rat and mouse Thy 1 antigen. The conjugates bind to the target cells specifically, but they did not lyse the target cells. They explained that the attachment of CytA to mAb molecule obstructed the pore-formation of cytolytic toxin leading to failure of cell lysis. Another conjugate was constructed by linking CytA toxin to insulin. However, the result showed that the cytolytic activity of CytA toxin is reduced when bound to the target cells (59).

CHAPTER II

OBJECTIVES

Many recent publications have reported that amino acid residue on the loop structure between α and β domain of Cyt2Aa2 involving the biological activity of the toxin. This thesis work aimed to investigate the effect of positively charge amino acid substitution, lysine, at the polar amino acid, asparagines and threonine, on the loop between α -helices domain and β -sheets domain of Cyt2Aa2 protoxin by using a site-directed mutagenesis. The mutant toxins, N89K and T148K, were designed and constructed by PCR based method. The resulting mutants were subjected to biochemical and biological assays. The results obtained from this study would provide the data for a better understanding of toxin structure and function as well as the mechanism of the toxin.

CHAPTER III

MATERIALS

3.1 Chemicals

| | |
|---|-----------|
| Acrylamide | Sigma |
| Ammonium Persulfate | Sigma |
| Ampicillin Disodium Salt | Bio Basic |
| Coomassie Brilliant Blue G 250 | USB |
| IPTG (Isopropyl β -D-1-thiogalactopyranoside) | USB |
| Sodium Dodecyl Sulfate (SDS) | Bio Basic |
| TEMED (N, N, N', N'-tetramethylethylenediamine) | Bio Basic |

Other chemicals and solvents were purchased from various suppliers (BIO-RAD, Merck and Sigma).

3.2 Bacteria strain

Escherichia coli strain JM109 [*recA1 supE44 endA1 hsdR17 gyrA96 rclA1 thi* Δ (*lac-proAB*) F' (*traD36 proAB⁺ lacI^q lacZ* Δ M15)] containing pGEM-Cyt2Aa2 plasmid (60) (**figure 9**).

3.3 Bacteria Culture Media

A liter of culture media are undefined medium of Luria-Bertani medium (LB) containing 1% (W/V) of Bacto-tryptone, 0.5% (W/V) of Bacto-yeast extract and 1% (W/V) of NaCl. In addition, 1.5% (W/V) of Bacto-agar was used into these components for preparing the culture plates (61). The media were sterile by autoclaving at 121°C, 15 psi. for 30 min. They were cool down to approximately 50-60°C and then added with ampicillin to the final concentration of 100 μ g/ml.

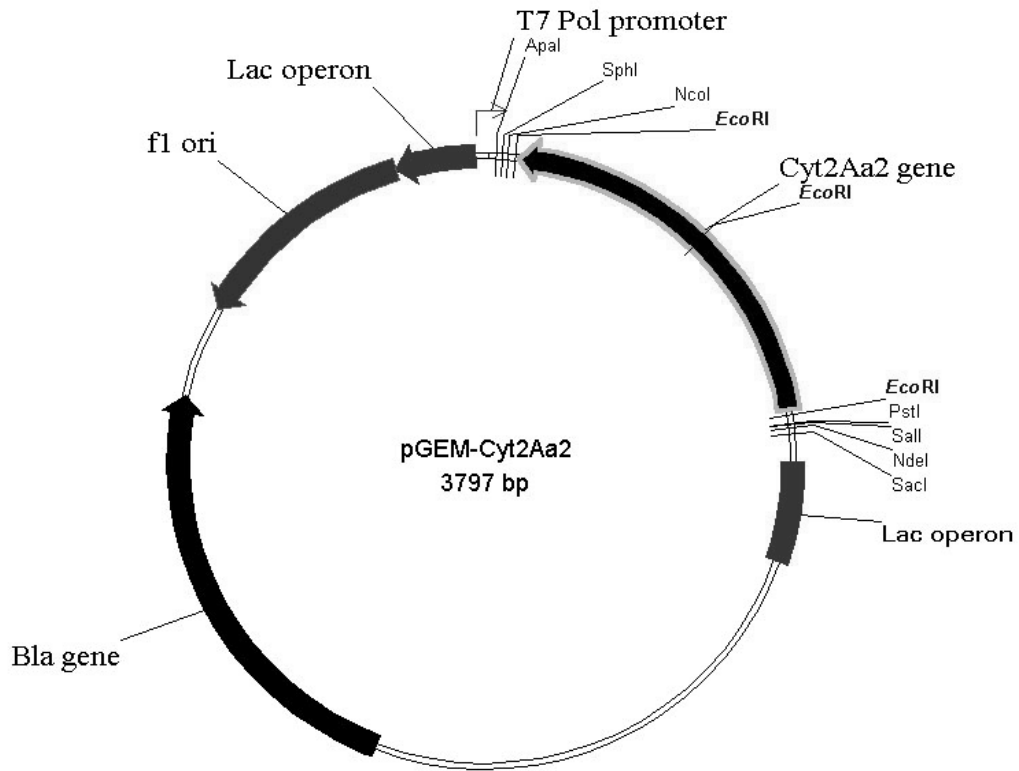


Figure 9: Map of the Plasmid pGEM-T_{easy} containing *cyt2Aa2* gene.

The figure shows the physical map of the recombinant plasmid pGEM-Cyt2Aa2 containing the full length of 29.2 kDa *cyt2Aa2* gene (850 bp).

3.4 Enzymes and Proteases

Restriction endonucleases and other enzymes were purchased from the following companies:

| | |
|---------------------------|---------|
| <i>Pfu</i> DNA polymerase | Promega |
| Hen egg Lysozyme | Sigma |
| RNase A | Sigma |

3.4.1 Proteases

| | |
|---|-------|
| Proteinase K | Sigma |
| Trypsin (Bovine pancreas, TPCK treated) | USB |

Chymotrypsin (Sigma) was supported by Dr. Boonhiang Promdonkoy, BIOTEC, National Science and Technology Development Agency, Thailand.

3.4.2 Restriction endonucleases

Table 2: List of restriction endonucleases and their recognition sites

| Enzyme name | Recognition Sites | Buffers | Companies |
|--------------|---|----------|-----------|
| <i>Cla</i> I | AT [▼] CG AT TA GC [▲] TA | Buffer C | Promega |
| <i>Dde</i> I | C [▼] TNA G G ANT [▲] C | Buffer D | Promega |
| <i>Dpn</i> I | G ^{me} A [▼] TG CT ^{me} [▲] AG | Buffer B | Promega |
| <i>Hha</i> I | G CG [▼] C C [▲] GC G | Buffer C | Promega |

Note: The cleavage site is specified by “ “ . ▼

Buffer B: 6 mM Tris-HCl, 6 mM MgCl₂, 50 mM NaCl, 1 mM DTT, pH 7.5

Buffer C: 10 mM Tris-HCl, 10 mM MgCl₂, 50 mM NaCl, 1 mM DTT, pH 7.9

Buffer D: 6 mM Tris-HCl, 6 mM MgCl₂, 150 mM NaCl, 1 mM DTT, pH 7.9

3.5 Oligonucleotide primers

The oligonucleotide primers were obtained from Proligo (Singapore). The sequences of the primers are shown below. Single code-amino acid letters were placed above their corresponding nucleotide sequences. Introduced restriction endonuclease recognition sites are underlined. The bold letters indicate the mutated nucleotides or amino acid residues.

Primer set 1: for sited-direct mutagenesis of pGEM-Cyt2Aa2, these oligonucleotide fragments were design to substitute Asparagine (N) at position 89 with Lysine (K).

I P **K** S A I V K T
N89K-F: 5'-ATT CCT AAG TCT GCA ATT GTA AAA ACT C-3'
DdeI

N89K-R: 5'-C AAT TGC AGA CTT AGG AAT ACC ATT TG-3'
DdeI

Primer set 2: for sited-direct mutagenesis of pGEM-Cyt2Aa2, these oligonucleotide fragments were design to substitute Threonine (T) at position 148 with Lysine (K).

L D **K** Q I D E A W
T148K-F: 5'-AT TTA GAC **AAA** CAA ATC GAT GAA GCA TGG-3'
Clal

T148K-R: 5'-GC TTC ATC GAT TTG **TTT** GTC TAA ATT TG-3'
Clal

3.6 Miscellaneous

| | |
|---|-----------|
| 5-Bromo-4-chloro-3-indolyl phosphate (BCIP) | Sigma |
| Alkaline phosphatase-conjugated anti-rabbit IgG | Sigma |
| Amicon [®] Ultra-4 centrifugal Filter Devices | Millipore |
| Bovine serum albumin, Bovine Albumin, BSA | Promega |
| Bradford protein assay reagent | BIORAD |
| Lambda DNA/ <i>HinD</i> III Markers | Promega |
| Nitro blue tetrazolium cholride (NBT) | Bio Basic |
| Precision Plus Protein [™] Standards (unstained) | BIORAD |
| SDS-PAGE molecular mass standards (board range) | BIORAD |
| Set of dATP, dCTP, dGTP, and dTTP | Promega |

Liposome (50) and Polyclonal antibody against Cyt2Aa2 were supported from Dr. Boonhiang Prodonkoy, BIOTEC, National Science and Technology Development Agency (NSTDA), Thailand.

CHAPTER IV

METHODS

4.1 DNA preparation using alkaline lysis (62)

The alkaline lysis has been a common method to isolate the plasmid DNA from *E. coli* cells for more than 30 years. The alkaline lysis method was performed according to Sambrook and Russell (61). A single colony of *E. coli* containing pGEM-Cyt2Aa2 plasmid was inoculated into 3 ml of LB broth with 100 µg/ml of ampicillin and incubated at 37°C for 16-18 hours. After overnight incubation, the culture was centrifuged at 12,000 rpm for 30 seconds in 1.5 ml microcentrifuge tube. Only cell pellet was resuspended in 100 µl of alkaline lysis solution I [50 mM glucose, 25 mM Tris-Cl (pH 8.0) and 10 mM EDTA (pH 8.0)] by vortex. A 200 µl of freshly prepared alkaline lysis solution II [0.2 N NaOH and SDS 1% (w/v)] was added into the mixture then the tube was inverted gently for 3-5 times. Subsequently, 150 µl of alkaline lysis solution III, which is the mixture of 60 ml of 5 M potassium acetate, 11.5 ml of glacial acetic acid and sterile distilled water 28.5 ml, was added to neutralize the pH value of the suspension. The mixture was mixed several times by inversion until the solution become viscous then keep the mixture at room temperature for 3-5 minutes. When incubation was complete, liquid phase was isolated from the mixture by centrifugation at maximum speed of 14,000 rpm for 5 minutes and transferred to a fresh tube. 2 µl of 10 mg/ml RNase was added into the supernatant for a removal of the contaminated RNA with incubation at 37°C for 1 hour. The protein contamination in liquid phase was eliminated by phenol: chloroform solution (phenol: chloroform: isoamyl alcohol, 25:24:1 v/v). An equal volume of phenol: chloroform solution was added into the mixture and vortex. The supernatant was separated by centrifugation at 14,000 rpm for 2 minutes and transferred to a new tube. This step was repeated one more time. To precipitate the plasmid DNA, two volumes of absolute ethyl alcohol was added into the solution, vortex and strand the

mixture at room temperature for 2 minutes. Then, centrifuged the mixture at the 14,000 rpm for 5 minutes and discarded the supernatant. Add 1 ml of 70% ethyl alcohol to the DNA pellet and inverse the tube several times. To recover the DNA plasmid, the mixture was centrifuged at 14,000 rpm for 2 minutes and discarded the supernatant. To remove the rest of ethyl alcohol, the microcentrifuge tube was placed upside-down on the paper towel until the pellet was dry. Finally, the DNA pellet was dissolved in 50 μ l of sterile distilled water and store at -20°C before use.

4.2 Agarose gel electrophoresis

Agarose gel electrophoresis is the basic method used for DNA analysis. DNA is analyzed on different percent of agarose upon the DNA size. Agarose powder was dissolved in 1X TBE buffer (90 mM Tris, 90 mM boric acid, 2 mM EDTA pH 8.0) and then boiled until the solution was in homogeneity using microwave oven. The gel solution was poured into electrophoretic tray when it is warm and allowed to solidify. DNA samples were mixed with DNA-loading dye [15% (w/v) Ficoll 400, 0.01% (w/v) Bromophenol blue] at ratio 1:5 (v/v) and then loaded into the well of submerged agarose gel in 1X TBE buffer. The electrophoresis was performed at a constant voltage of 100. After electrophoresis completed, the gel was stained in ethidium bromide solution for 5 min and destained in distilled water for 20 min or until the background was clear. The stained DNA patterns were visualized under UV light (Gel Doc model 1000, Bio-Rad, USA) and a photograph is taken.

4.3 Site-directed mutagenesis

Site-directed mutagenesis is the mutagenic method based on the Quick Change™ Site-directed Mutagenesis Kit (Stratagene) (**figure 10**). The pGEM-T vector (promega) containing full length *cyt2Aa2* gene from *B. thuringiensis* subsp. *darmstadiensis* (a gift from Dr. Boonhiang Promdonkoy) was a subject to be mutated in this experiment. Two sets of oligonucleotide were used as the primer to substitute asparagine at position 89 or threonine residue 148 with lysine (**figure 11**). The first primer set to substitute asparagine residue 89 with lysine was designed to have nucleotide on the DNA sequence of *cyt2Aa2* changed from AAT to AAG. It also has an additional recognition site of *DdeI*. Another pair of primer that mutate threonine

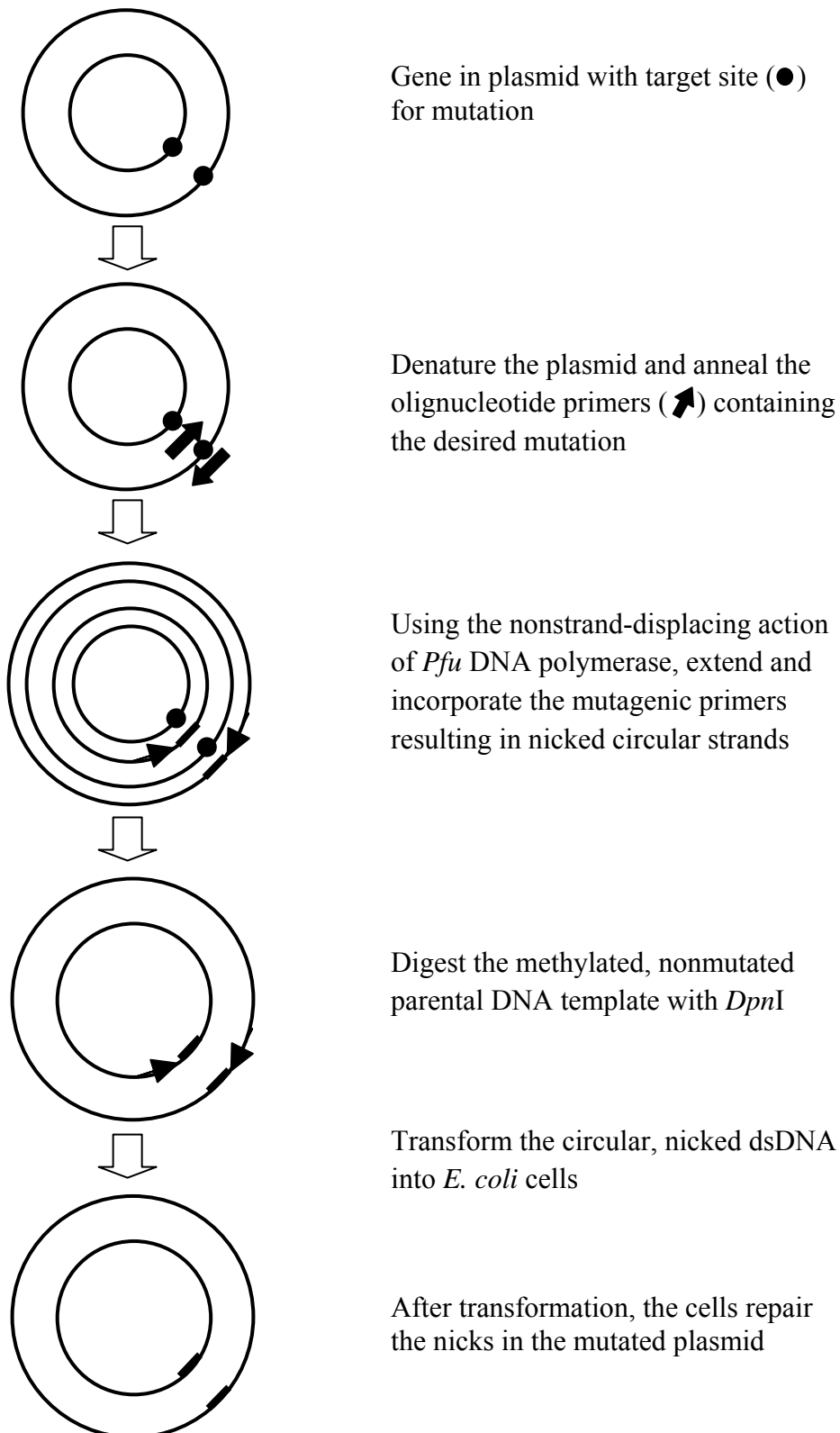


Figure 10: Overview of QuikChange™ site-directed mutagenesis method (Stratagene).

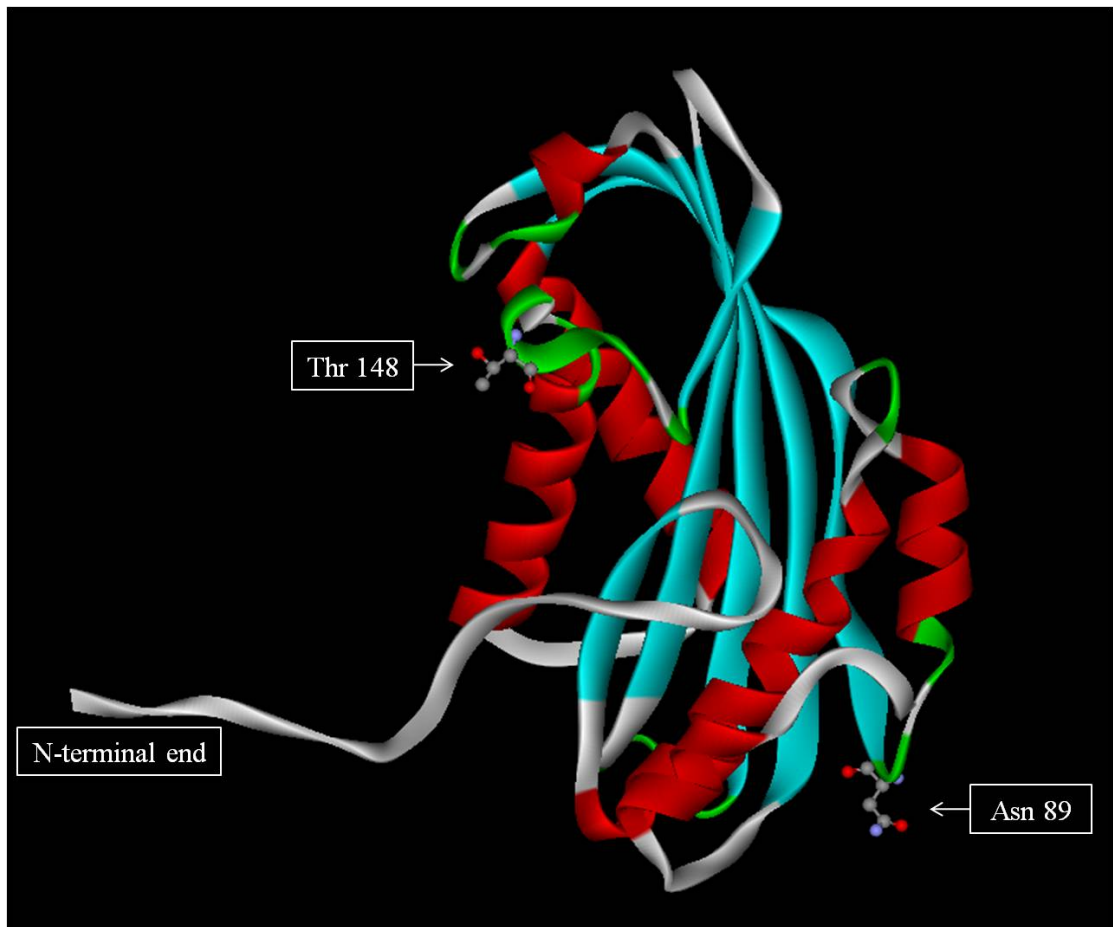


Figure 11: Position of Asn 89 and Thr 148 on the three dimensional structure of Cyt2Aa2 toxin. (constructed by WebLab Viewer program)

position 148 to lysine was designed to have codon change from ACT to AAA. Since this primer set did not create or remove the restriction site that can be used to identify the mutant, thus adenine was replaced with cytosine to produce a *ClaI* recognition site. The whole sequence of these primers and their complementary were shown in part of materials.

An automated GeneAmp PCR System 2400 thermal cycler (Perkin-Elmer, CA, USA) was used to perform PCR reactions for all samples. The reactions were done in 200- μ l thin wall PCR tubes. PCR reaction mixture (50 μ l) was consisted of :

| | |
|--|---------------|
| DNA template | 50 - 100 ng |
| 10 mM dNTP mix (2.5 mM each) | 1 μ l |
| Forward and reverse primers | 10 pmole each |
| 10x <i>Pfu</i> buffer | 5 μ l |
| <i>Pfu</i> DNA polymerase | 1 μ l |
| Sterile distilled water making final volume to | 50 μ l |

After PCR reaction was performed (depending on the primer sets as shown in **Table 3**). The DNA-template was digested by *DpnI*. 20 μ l of each PCR product was analyzed on 0.8% (w/v) agarose gel.

4.4 The template elimination by *DpnI* digestion

For a removal of DNA-plasmid template, 1 μ l of *DpnI* restriction enzyme (10 units/ μ l) was added into the PCR product and incubate the mixture at 37°C for 2 hours. The *DpnI* restriction endonuclease is ‘four cutters’ enzyme that target the methylated and hemimethylated nucleotide strand isolated from almost all *E. coli* strain. Therefore only the parental DNA template will be digested and yield the nicked mutant DNA plasmid. A 20 μ l of each digested product was analyzed on 0.8% agarose gel before a transformation into competent *E. coli* cells.

4.5 Introduction of DNA plasmid into *E. coli* using heat-shock method (61)

A 200 μ l of frozen MgCl₂-CaCl₂ treated competent cells was thawed and gently mixed with 5-10 μ l of the PCR product. The contents were left on ice for 30 minutes and dip in 42°C for 90 seconds immediately. Then the mixture was left on ice for 5 minutes. 800 μ l of non-antibiotic LB media was added into the mixture and

Table 3: Temperature cycling parameters for site-directed mutagenesis.

| Primer set | Template | Segment | Cycle | Temperature | Time |
|-----------------------------|-------------|---------|-----------|--------------|-----------------------|
| N89K-F,R or T148K-F,R | pGEM-Cyt2Aa | 1 | 1 | 95°C | 1 seconds |
| | | 2 | 20 | 95°C | 30 seconds |
| | | | | 45°C 72°C | 1 minute 8 minutes |
| 3 | 1 | 72°C | 8 minutes | | |

culture at 37°C for 1 hour. After that, the transformed cells were separated by centrifugation at 7,000 rpm for 5 minutes and resuspended in 200 µl of LB broth. Finally, the suspension was spread on antibiotic LB agar plate and incubated at 37°C for overnight.

4.6 Preparation of competent cells by MgCl₂-CaCl₂ (61)

A single *E. coli* colony was inoculated in 100 ml of LB broth with 100 µg/ml ampicillin at 37°C until the OD₆₀₀ is 0.4. Then 50 ml of cell culture was transferred into centrifugal tubes and packed at 2,700g for 10 min at 4°C. The cell pellet was gently resuspended in 30 ml of ice-cold MgCl₂-CaCl₂ solution (80 mM MgCl₂, 20 mM CaCl₂) while the supernatant was removed. The cells were recovered by centrifugation again and resuspended softly in 2 ml of ice-cold 0.1 M CaCl₂ solution. The competent cells were stored in 30% Glycerol and aliquot of 200 µl of competent cells was stored at -70°C until use.

4.7 Screening for the mutated clones

4.7.1 Mutant screening by restriction enzyme analysis

To screen for the N89K mutant clone, 200 ng of the plasmids from each transformed clone was extracted by alkaline lysis method (method 4.1) and digested with 1 µl of *DdeI* restriction endonuclease. The *ClaI* and *HhaI* double digestion was also performed to screen for T148K mutant clone. Both reactions were incubated at 37°C for 1 hour and analyzed on 1.2% agarose gel electrophoresis as previously described.

4.7.2 Automated DNA sequencing analysis

To confirm the DNA sequence of the mutant clones, the DNA plasmids were extracted by alkaline lysis method (method 4.1) and their polynucleotide sequence of *cyt2Aa2* gene were analyzed by MegaBACETM 500 Automated DNA sequencer (Amersham Pharmacia Biotech, USA) using M13 universal forward and reverse primers. The sequencing results of DNA plasmid were compared with DNA sequence of wild-type *cyt2Aa2* using AlignX software in Vector NTI Suite 8.

4.8 SDS-Polyacrylamide Gel Electrophoresis (SDS-PAGE)

4.8.1 SDS-PAGE analysis using coomassie blue staining

SDS-PAGE is a method to analyse the proteins according to their electrophoretic mobility. The SDS-PAGE was composed of separating and stacking gel. The stacking layer composes of 2.6% C, 4% T, 0.125 M Tris-HCl pH 6.8 and 0.1% SDS. The separating layer contains 2.6% C, 10% or 13% T, 0.375 M Tris-HCl pH 8.8 and 0.1% SDS. Running buffer is Tris-glycine buffer (25 mM Tris, 192 mM glycine, 0.1% SDS).

For protein sample preparation, the protein samples were mixed with 4X sample buffer and heated at 95°C for 5 minutes. Then the samples were spun down and loaded on SDS-PAGE. Electrophoresis was performed by constant voltage 150 V at room temperature until the dye from 4X sample buffer reached bottom of the gel. The protein bands were visualized by staining the gel in colloidal Coomassie blue (100g of Ammonium Sulfate, 20 ml of H₃PO₄, 1 g of Coomassie Blue G-250, and added H₂O to 1,000 ml) for overnight with tender shaking. After that, the gel was destained in distilled water overnight or until the background was clear.

4.8.2 Silver staining of SDS-PAGE gel

After performing the SDS-PAGE, the protein samples were fixed on the gel by submerging in fixed solution [methanol alcohol 50% (v/v), acetic acid 12% (v/v)] for 1 or 2 hours at room temperature. If the gel was already stained with coomassie dye, the gel would be submerged in fixed solution until the gel was clear. The gel was washed twice with washing solution [ethanol alcohol 35% (v/v)] for 20 minutes each. The gel was then washed with Milli-Q water for 10 minutes and sunk in fresh sensitizing solution [Na₂S₂O₃ 0.02% (w/v)] for 2 minutes. And the gel was washed twice with Milli-Q water for 5 minutes each. The gel was stained in silver nitrate solution [AgNO₃ 0.2% (w/v), formaldehyde 0.076% (v/v)] for 20 minutes. After staining, the gel was washed again with Milli-Q water for 1 minute. Then the gel was colorized in developer [Na₂CO₃ 6% (w/v), formaldehyde 0.05% (v/v), Na₂S₂O₃ 0.0004% (v/v)]. Until the protein bands were appeared well, the gel was sunk in stopping solution [methanol alcohol 50% (v/v), acetic acid 12% (v/v)] for 5 minutes to terminate the

reaction. The stained SDS-PAGE was stored in 4% acetic acid or packed in plastic bag at 4°C.

4.9 Protein concentration assay using Bradford reagent

The concentration of soluble protein was determined by using Bio-Rad protein assay based on the method described by Bradford (63). The standard curve was constructed by using Bovine Serum Albumin (BSA) as a protein standard. BSA was diluted into 6 concentrations ranging from 0, 0.1, 0.2, 0.4, 0.6, 0.8 mg/ml. A 10 µl of the proteins was mixed with 300 µl of dye solution in 96-well microtiter plate. The mixtures of protein-dye were incubated at room temperature for 5 min. The absorbance was analyzed by wavelength at 595 nm, using ELISA plate reader (SpectraMAX190, Molecular Devices). The concentration and quantity of proteins were calculated from standard curve.

4.10 Western blot analysis

After the protein samples was separated by SDS-PAGE, the separating gel containing resolved protein bands was equilibrated in the transfer buffer (39 mM glycine, SDS 0.04% (w/v), methanol 10% (v/v) and 48 mM Tris-HCl, pH 9.2) for 10 minutes. For one gel, a piece of nitrocellulose membrane and 6 pieces of Whatman® paper were cut to the same size as the gel and equilibrated in the transfer buffer for 10 minutes. Protein samples were electrophoretically transferred from the gel to a nitrocellulose membrane using a semi-dry blot apparatus (Multiphor II electrophoresis system, Pharmacia Biotech). The 3 pieces of Whatman® paper were placed on the graphite electrode and the stack of nitrocellulose membrane, the gel and another 4 pieces of Whatman® paper was placed on top of that respectively. The electroblotting was carried out at current constant at 3 mA per cm² of gel for one and a half hours. The nitrocellulose was then washed in 1x PBS buffer (120 mM NaCl, 16 mM Na₂HPO₄·2H₂O, 4 mM KH₂PO₄, pH 7.4). In order to block non-specific binding of antiserum, the membrane was submerged in blocking solution [5% (w/v) skim milk in 1x PBS buffer, pH 7.4] for overnight with rocking at 4°C. To detect the Cyt2Aa2 fragment, the rabbit anti-Cyt2Aa2 polyclonal antibody was added into the fresh blocking solution at the dilution 1:10,000 and incubated at room temperature for 1

hour with rocking. Then the membrane was washed three times with 1x PBS containing 0.1% tween-20 for 5 minutes each time. After that the membrane was incubated with the secondary antibody (alkaline phosphatase-conjugated anti-rabbit IgG) in 1x PBS and 5% skim milk with the dilution 1:10,000 at room temperature for 30 minutes. The membrane was washed once with 1x PBS containing 0.1% tween-20 for 5 minutes and washed three times with 1x PBS for 5 minutes each time. The immuno-reactive bands on the membrane were detected by incubating in carbonate buffer (1 mM MgCl₂.6H₂O and 100 mM Na₂CO₃, pH 9.8) containing the developer solution [5-bromo-4-chloro-3-indolyl phosphate/ nitroblue tetrazolium (BCIP/NBT)] until a band was seen. After the color reaction was complete, the membrane was rinsed with tap water and kept dry in a dark envelope.

4.11 Cytolytic protoxins preparation

A single colony of the mutant was inoculated in 15 ml of LB broth containing 100 µg/ml of ampicillin at 37°C for overnight. The overnight culture was transferred into 700 ml of fresh LB media with ampicillin and incubated at 37°C until the OD₆₀₀ is 0.4-0.5. Then, the protein expression was induced by IPTG at final concentration of 0.1 mM and continued incubation for 5 hours at 37°C. Next, the cells were harvested using centrifugation at 6,000 rpm, 4°C for 20min. The cell pellet was suspended with 30 ml of sterile distilled water. To find out the protein expression level of *E. coli*, the 1 OD₆₀₀ of *E. coli* cells were collected by centrifugation 14,000 rpm for 30 sec. The cell pellet was resuspended with 50 µl of sterile distilled water and 20 µl of 4X sample buffer. The sample mixture was boiled at 95°C for 5 minutes and analyzed 8 µl of the mixture on 12.5% SDS-PAGE (method 4.8.1).

The cell resuspension was incubated with 20 µl of 100 mg/ml lysozyme and incubated at room temperature for 2 hours or at 37°C for 5-10 minutes. After that, the cells were lysed using the French Pressure Cell (64) at 10,000 psi for three times. Then, the insoluble was isolated from the cell lysate by centrifugation at 8,000 rpm, 4°C for 15 minutes. The inclusion bodies were partially purified by washing with 30 ml of ice-cold sterile distilled water for three times (65). Lastly, the partially purified inclusions were suspended in 3 ml of sterile distilled water and aliquots of 1 ml of inclusion were stored at -20°C until use.

4.12 Protoxin solubilization and proteolytic processing

Before proteins were solubilized in 50 mM carbonate buffer at pH 10.8, they were centrifuged at 12,000 rpm, 4°C for 10 minutes and discarded the supernatant. The inclusion pellet was incubated with the 50 mM carbonate buffer at 37°C for 1 hour. The solubilized protein was isolated from the solution by centrifugation at 4°C, 12,000 rpm for 10 minutes. Then the proteins were analyzed on SDS-PAGE.

The solubilized protein was digested with proteinase K at a 1:100 (w/w) ratio of protease: total protein (60). A mixture of protein and protease was incubated at 37°C for 1 hour. For other preparations, the solubilized protein was also activated by chymotrypsin at a 1:50 (w/w) for 2 hours at 37°C. The enzyme activity was then inhibited by adding phenylmethane sulfonyl fluoride (PMSF) at a final concentration of 4 mM. The digested products were analysed on 15% SDS-PAGE. Furthermore, some solubilized protein was subject to digested with the 5% (w/w) TPCK treated trypsin at 37°C for 3 hours.

4.13 Protein purification using Superdex™ 200

The Superdex™ 200 HR 10/30 column is the size exclusion column which separates proteins or peptides in the molecular weight range of 10-600 kDa. Before using the column, the column had to be connected to ÄKTA Purifier System under Unicorn 3.0 computer controlling software (Amersham Pharmacia Biotech, USA). Column equilibration was performed with filtered sterile Milli-Q water and 50 mM of carbonate buffer at pH 10.8. The protein sample was centrifuged at 12,000 rpm, 4°C for 10 minutes to prepare the sample for injection. After injection of 0.4 ml of the protein sample, the purification was performed at flow rate 0.4 ml/min. The purified profile was observed by UV absorption at 280 nm. The protein from each peak was collected and analysed on SDS-PAGE. After using the column, the column was equilibrated with Milli-Q water and store in 20% ethanol alcohol.

4.14 Protein concentration assay using UV-absorption spectroscopy

UV-absorption of peptide bonds at far-UV region can be used to determine a concentration of purified protein as described by Waddell (66). The protein solution was applied in a quartz cuvette (JASCO). UV absorption was scanned from 190-350

nm using Cary300 Bio UV-Visible spectrophotometer (Varian, Australia) under controlled of Cary Win-UV software. The absorption of 50 mM Na₂CO₃/NaHCO₃ buffer pH 10.8 was subtracted from the protein spectrum. Absorption baseline was corrected. The following equation was employed to calculate the protein concentration in the unit of mg/ml.

$$\text{Protein concentration} = 0.144 \times (\text{OD}_{215} - \text{OD}_{225}) \times \text{dilution factor} \quad (4.14.1)$$

The OD₂₁₅ and OD₂₂₅ are the optical density at the wavelength of 215 nm and 225 nm, respectively. The cuvette path length was 1 cm.

4.15 Tertiary structure analysis using intrinsic fluorescence spectroscopy

The fluorescence spectroscopy was used to analyze for structural changes of the purified proteins. The fluorescence spectra were obtained by emission scanning of approximately 0.04 mg/ml toxin in quartz cell with 0.5 cm path length using the JASCO FP-6300. All measurements were performed at room temperature with excitation wavelength at 280 nm. The emission spectra were recorded from 300-500 nm and the background spectrum was subtracted from the protein spectrum.

4.16 Larvicidal activity assay

2-days old *A. aegypti* larvae were used for toxicity assay (60). The larvae were obtained from the mosquito-rearing facility (Institute of Molecular Biology and Genetics, Mahidol University). The inclusions proteins were prepared as the 2-fold serial dilution and fed to the larvae in 24-wells titer plate. Each dilution of inclusions was adjusted the volume to 1 ml with distilled water, then added to 1 ml of distilled water containing 10 mosquitoes larvae. In this experiment, one hundred mosquito larvae were used for one experiment and each experiment was repeated at least 3 times. The mortality was recorded and analyzed after 24 h of incubation at room temperature.

4.17 Hemolytic activity assay

Hemolytic activity assay were performed in 96-well microtiter plate using Sheep Red

Blood Cells (60). The sheep RBCs were purchased from National Laboratory Animal Centre, Mahidol University, Salaya Campus. Before performing the assay, the sheep blood was washed with 1X PBS buffer (8 mM Na₂HPO₄, 1.5 mM KH₂PO₄, 140 mM NaCl, 2.7 mM KCl, pH 7.4) (Sambrook) until the supernatant was clear. Then the blood cells were collected by centrifugation at 3,000 rpm, 4°C for 5 minutes and diluted in PBS buffer to prepare 2% (v/v) sheep RBCs. Hemolytic activity assay was performed by 2-folds serial dilution of active toxin by PBS buffer. After performing the dilution series in microtiter plate, 100 µl of 2% sheep RBCs were mixed with 100 µl of active toxin dilution then keep at room temperature. The end point of hemolytic activity was recorded after overnight incubation.

4.18 Hemoglobin release assay

Hemoglobin release assay is a method that directly measures the hemoglobin released from the red blood cells by measuring the absorbance at 540 nm (65). The red blood cells were prepared similar to the hemolytic activity assay but the RBCs used was 1% (v/v). The 500 µl of sheep blood was incubated with 500 µl of the dilution of active toxin and incubated at room temperature for 1 hour. After incubation, the hemoglobin released from the RBCs was isolated by centrifugation at 12,000 rpm, 4°C for 30 seconds and then the supernatant was analyzed at wavelength of 540 nm, using ELISA plate reader (SpectraMAX190, Molecular Devices).

4.19 Oligomerization assay

The oligomerization of Cyt2Aa2 protein and the mutants were assayed by incubation with lipid vesicle or liposome (supported by Dr. Boonhiang Promdonkoy BIOTEC, National Science and Technology Development Agency, Thailand). 5 µg of active toxin was mixed with 200 µg of liposome in 1X PBS at pH 7.4 and incubated at room temperature for 2 hours. Then the mixture was centrifuged at 20,000 xg, 4°C for 20 minutes. Only the pellet was prepared to analyze on 12.5% SDS-PAGE by mixing with 20 µl of 2X sample buffer without sample boiling. The SDS-PAGE gel was stained with colloidal coomassie blue and silver nitrate reagent.

4.20 MTT cytotoxicity assay

The MTT assay is an indirect cell viability assay using tetrazolium-dye based colorimetric reaction (67). The yellow tetrazolium dye is reduced to blue formazan by mitochondria reductase. The metabolically deficient cells will assume to be not survived. The color change is measured by spectrometrically with a plate reader. The mutant toxins were test with four cell lines, 1) BHK(21)C13; a baby hamster kidney fibroblast, 2) IEC6; a rat small intestine epithelial, 3) HepG2; a human hepatocarcinoma, and 4) C6/36; a whole mosquito larvae of *Aedes albopictus*. The culture of BHK(21)C13 was Glasgow Modified Eagle's Medium (GMEM). The IEC was grown in Dulbecco's Modified Eagle's Medium (DMEM). The HepG2 and C6/36 were grown in Minimum Essential Medium (MEM). Before the toxins adding, cell lines were seeded in a 96-wells plate, and incubated at 37°C, for 48 hrs in a fully humidified, 5% CO₂:air atmosphere. The serial dilutions of the toxins were added to the cells and continue incubation for 24 hrs, then the cells were reincubated for another 24 hrs. in fresh medium and test with MTT assay. The absorbance at 570 nm was measured by microplate reader (Molecular Devices). Then the data were analyzed with the SoftMax Program (Molecular Devices) to determine the 50% inhibitory concentration (IC₅₀) for each sample.

CHAPTER V

RESULTS

5.1 The construction of mutant toxins

The *DpnI*-digested products were analyzed on 1.2% agarose gel electrophoresis. The PCR products of N89K and T148K showed a single band at 3.8 kb on the agarose gel (**figure 12**). Then the *DpnI*-digested products were transformed into *E. coli* JM109 competent cells.

To screen for mutant colony, the transformed colonies were extracted for DNA and analyzed by the restriction enzyme analysis. The pattern of DNA fragments was visualized on 1.2% agarose (**figures 13 and 14**). The *DdeI*-digested wild-type plasmid showed 4 fragments which are 2.6 kb, 540 bp, 409 bp and 166 bp. While the *DdeI*-digested N89K mutant gave 5 fragments at 1.4 kb, 1.2 kb, 540 bp, 409 bp and 166 bp. When the wild-type plasmid was analyzed with *ClaI* and *HhaI* double digestion provided 20 bands, whereas T148K mutant showed two more extra bands at about the 1.2 kb fragment of wild-type (**figure 14**). The pattern of restriction analysis predicted by computer program was found in good agreement with the obtained patterns. After restriction enzyme analysis, the plasmids extracted from the same clone were subjected to DNA sequence verification using automated DNA sequencing (**figures 13 and 14**). The universal M13 forward and reverse primers were used in the reactions. The chromatogram showed that the DNA sequence of each mutant clone was changed corresponding to the designed primers.

5.2 Protein production and solubility

The *E. coli* cells contained mutant plasmids were expressed upon induction with IPTG. After mutant protein harvesting, the cell lysates were loaded on 12.5% SDS-PAGE gel (**figure 15**). The inclusion bodies of protoxin of Cyt2Aa2 showed a molecular mass of 25 kDa. In addition, minor variation of protein expression was also

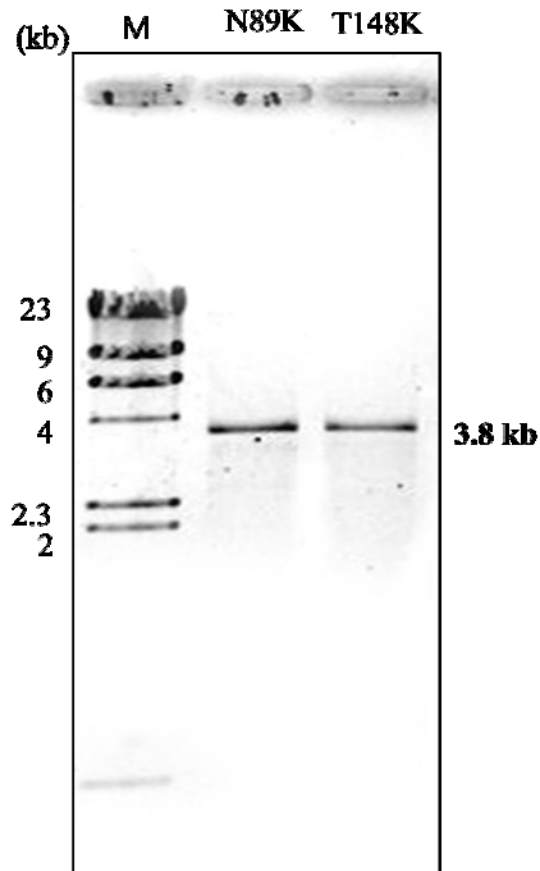


Figure 12: Amplification of N89K and T148K mutant plasmids

The PCR products of N89K and T148K mutants were constructed by site-directed mutagenesis with specific primers. Then PCR products of both mutant were digested with *DpnI* and analyzed on 1.2% agarose gel electrophoresis. M is λ /*HindIII* DNA marker. N89K is PCR product amplified by N89K primers. T148K is PCR product amplified by T148K primers. Both of them show a single band at 3.8 kb as expected.

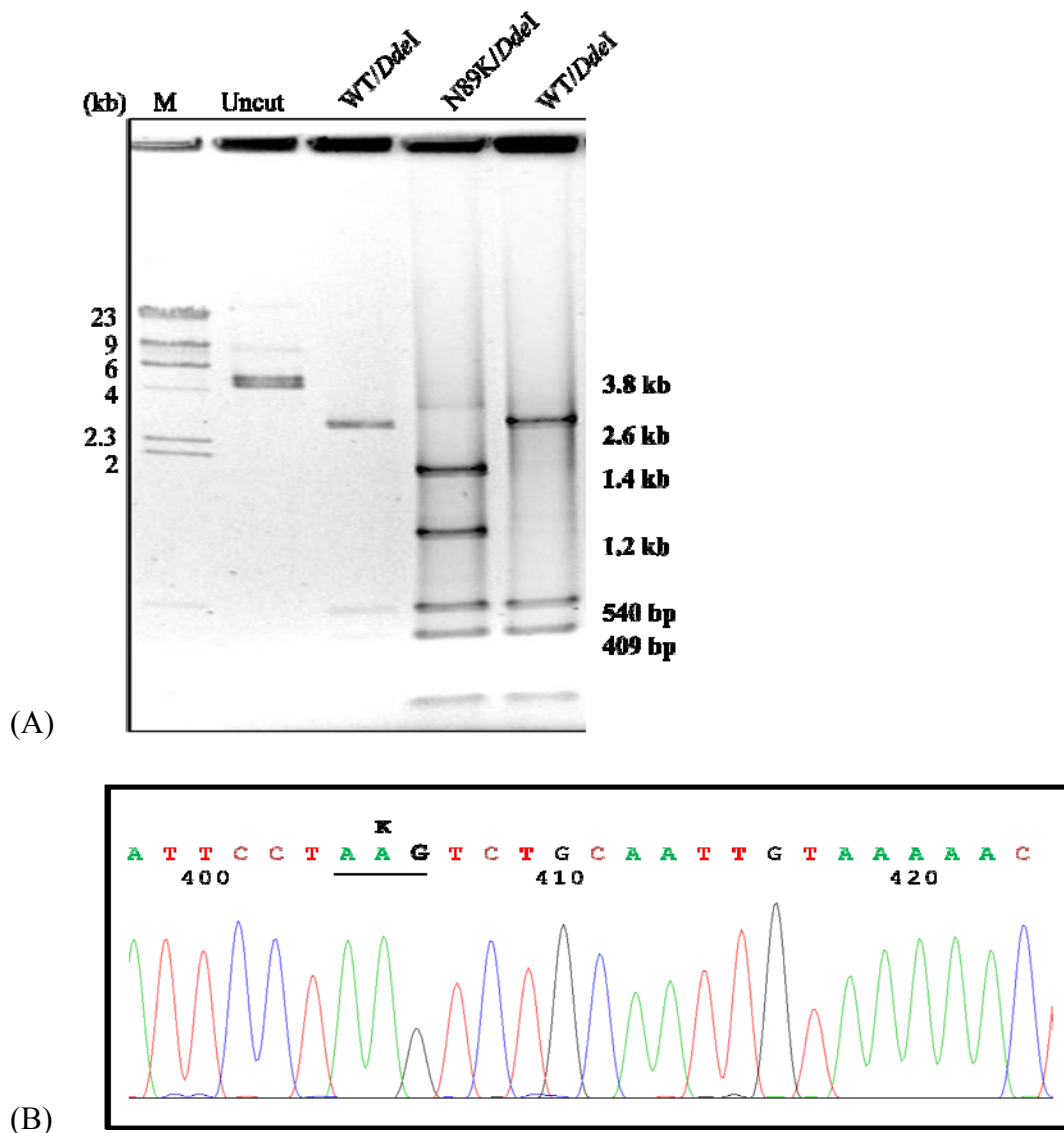


Figure 13: Restriction enzyme analysis and DNA sequencing of N89K mutant

The 1.2% agarose gel (A) shows the restriction map of N89K after digestion with *DdeI* (N89K/*DdeI*). λ /*HindIII* DNA marker and non-digested wild type plasmid were run in M and Uncut. *DdeI*-digested wild type plasmids are WT/*DdeI*. (B) is the chromatogram of N89K, using M13 as a sequencing primer. Part of the sense strand sequence is shown. The bold letter represents the substituted nucleotide and the underline corresponds to a amino acid codon of lysine.

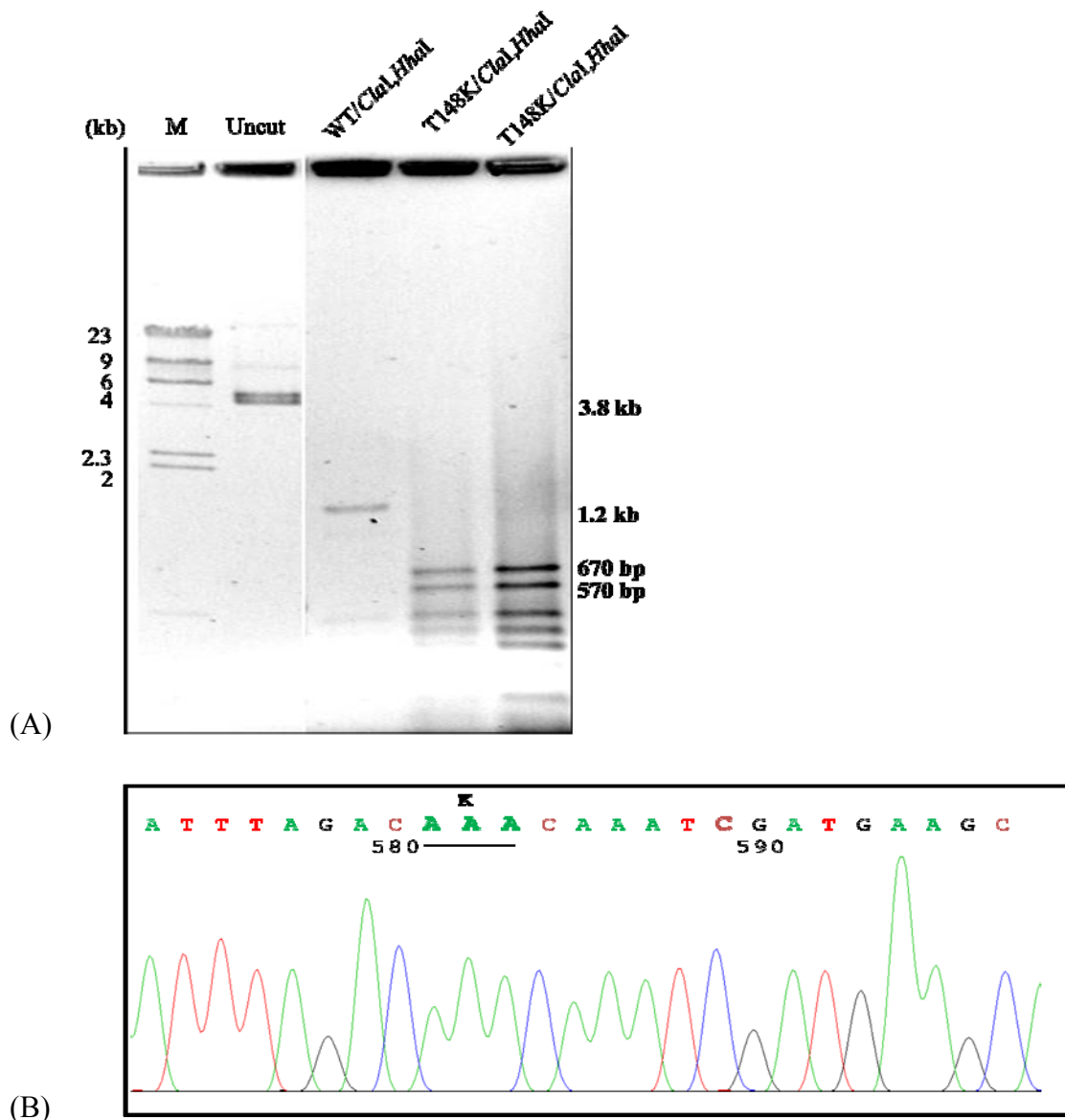
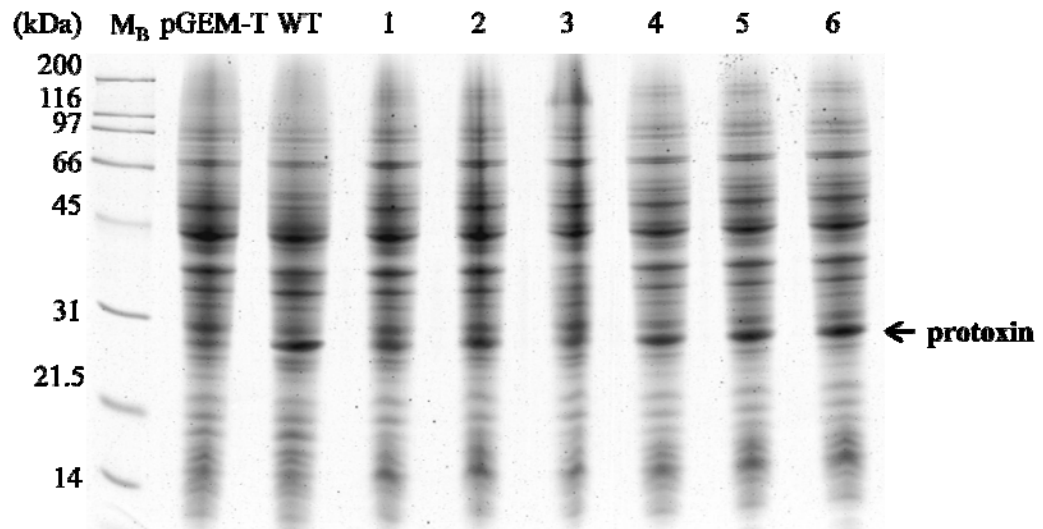
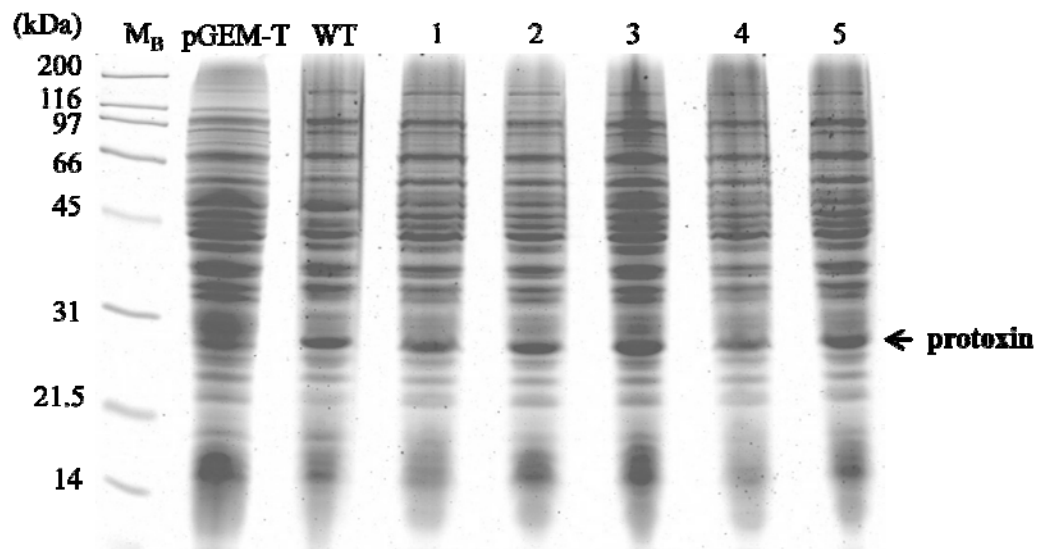


Figure 14: Restriction enzyme analysis and DNA sequencing of T148K mutant

The 1.2% agarose gel (A) shows the restrictoin map of T148K after digestion with *ClaI* and *HhaI* (T148K/*ClaI,HhaI*). λ /*HindIII* DNA marker and non-digested wild type were run in M and Uncut. The wild type plasmids digested with *ClaI* and *HhaI* are WT/*DdeI*. (B) is the chromatogram of T148K, using M13 as a sequencing primer. Part of the sense strand sequence is shown. The bold letter represents the substituted nucleotide and underline correspond to a amino acid codon of lysine.



(A)



(B)

Figure 15: The protein expression of N89K and T148K mutant

The figures show SDS-PAGE profiles (Coomassie Blue G staining 12.5% gel) of the whole cell lysates of 0.1 OD of IPTG-induced *E. coli* cells harboring from mutant N89K (A) and T148K(B). Lane M_B represents the broad-range protein marker and lane 1 to 6 are referred to clone number 1 to 6, respectively. WT and pGEM-T are the expression of wild type toxin and pGEM-T vector.

found between each clone. Only the *E.coli* clones expressing high level of product were selected for further experiments (clone number 4 for N89K mutant and clone number 3 for T148K mutant). Solubility of the mutant proteins in carbonate buffer, pH 10.8 was analyzed on 12.5% SDS-PAGE gel. The solubility of N89K is comparable to that of wild type while T148K is poorer than wild type about 2 or 3 times. Furthermore, the supernatant of inclusion washing was also analysed on 12.5% SDS-PAGE gel comparing with the whole cell lysate and inclusion (**figure 16**). Then the inclusion was transferred from SDS-PAGE gel to nitrocellulose membrane and probed with anti-Cyt2Aa2 IgG (**figure 17**). The result revealed that the anti-Cyt antibody could recognize the major band at about 25 kDa, and other faint bands at 10 and 50 kDa.

5.3 Proteolytic processing of mutant toxins

The inclusion bodies of wild-type, N89K, and T148K were solubilized in carbonate buffer, pH 10.8 and analyzed on 12.5% SDS-PAGE gel (**figure 18**). The equal amount of solubilized proteins of wild-type and mutants were subjected to digestion with proteinase K or chymotrypsin (**figure 19**). The digested products were analyzed on 12.5% SDS-PAGE gel. The results show that each digestion gave the product about 23 kDa. The amount of digested band were decreased after digestion with proteinase K, while the chymotrypsin digestion did not reduce the amount of digested protein.

5.4 Protein purification by size exclusion chromatography

The proteinase K activated toxin were purified by size exclusion chromatography. The chromatographic profile (**figure 20**) of purification was monitored from the absorbance at 280 nm as shown in Figure 8. Each peak from the profile was analysed on 12.5% SDS-PAGE gel as shown in **figure 21**. From the result, it is found that the activated Cyt2Aa2 protein (23 kDa) was eluted in peak number 3. For the N89K and T148K mutant, the activated protein were also eluted from the column at the same column volume as Cyt2Aa2 wild-type.

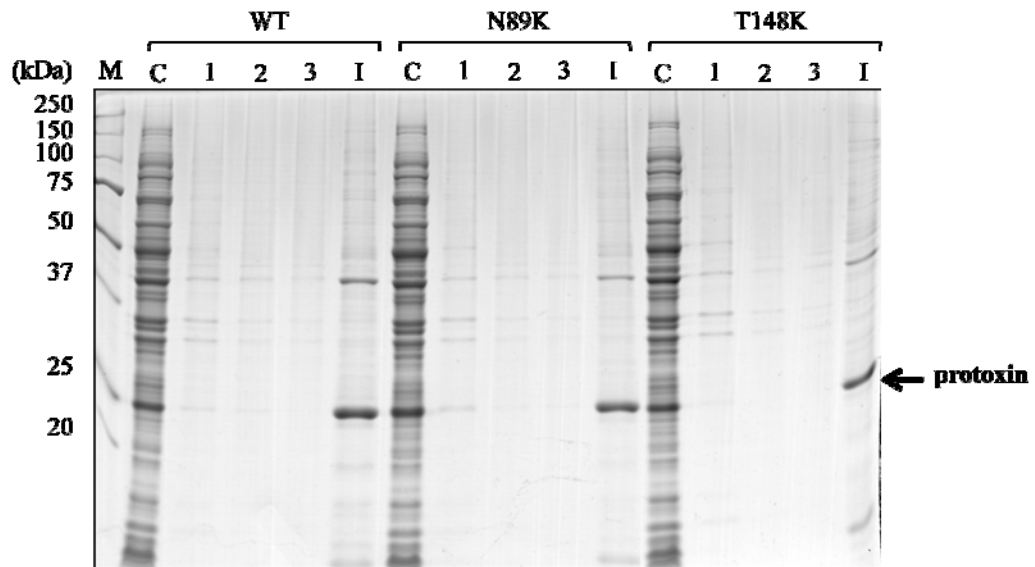


Figure 16: 12.5% SDS-PAGE gel of Cyt2Aa2, N89K, and T148K mutants compared with their washing solution. (M: precision protein marker, C: whole cell lysate, Lane 1-3: inclusion washing supernatant, and I: partially purified inclusion.)

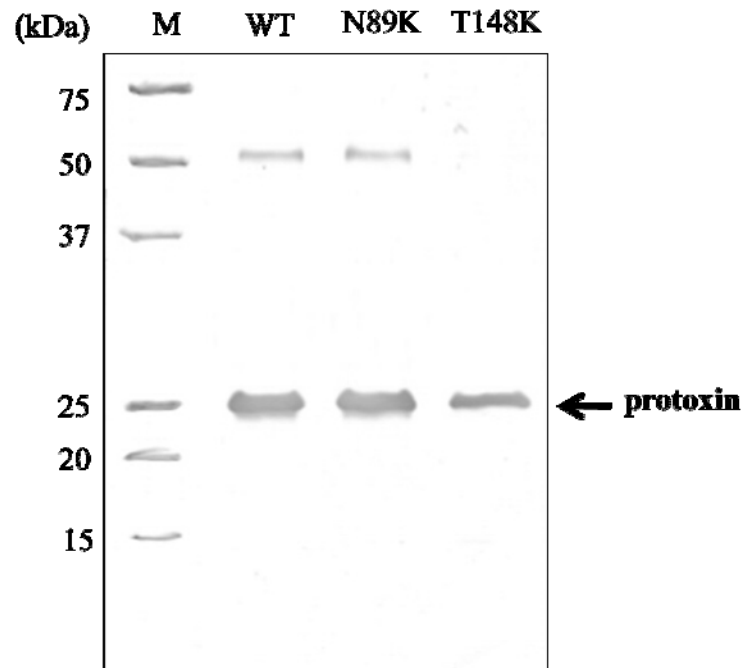


Figure 17: Western blot analysis of Cyt2Aa2, N89K and T148K protoxin.

The protein samples were run on 12.5% SDS-PAGE and transferred to nitrocellulose membrane. Then the Cyt2Aa2 protoxins were detected by polyclonal anti-Cyt2Aa2 antibodies. M is precision protein marker.

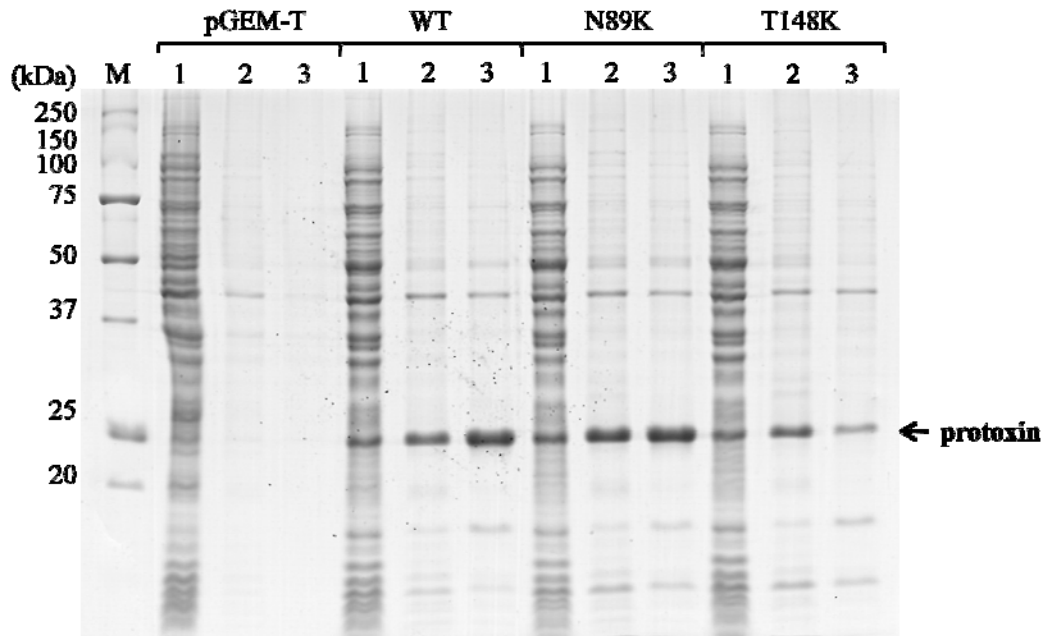


Figure 18: The protein expression and solubility of the mutant toxins.

The figure shows the whole cell lysate, partially inclusion and solubilized toxin are run in lane 1, 2 and 3. The precision protein marker was loaded in lane M.

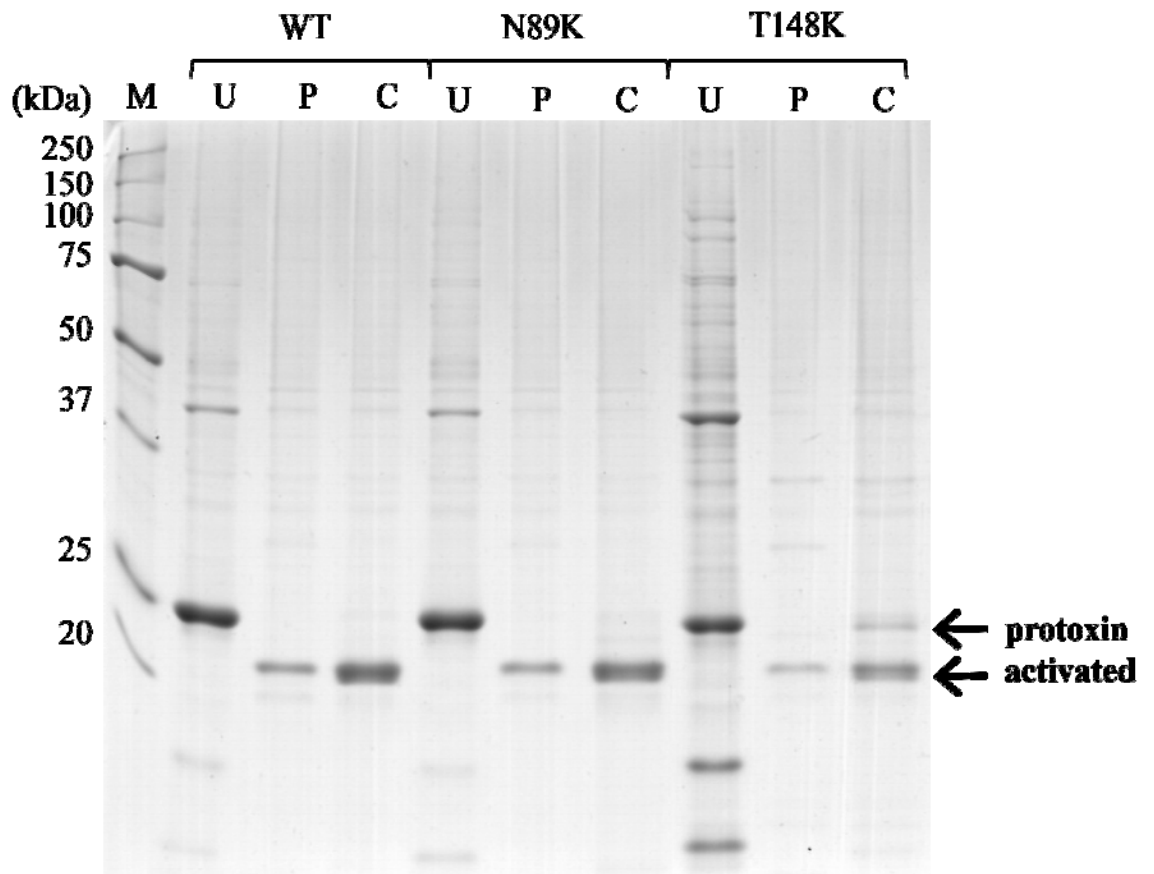


Figure 19: Proteolysis profile of proteinase K and chymotrypsin digestion.

M: precision protein marker. U: carbonate buffer solubilized Cyt2Aa2, N89K and T148K. P: proteinase K activation of WT, N89K and T148K. and C: chymotrypsin activation of WT, N89K and T148K, respectively.

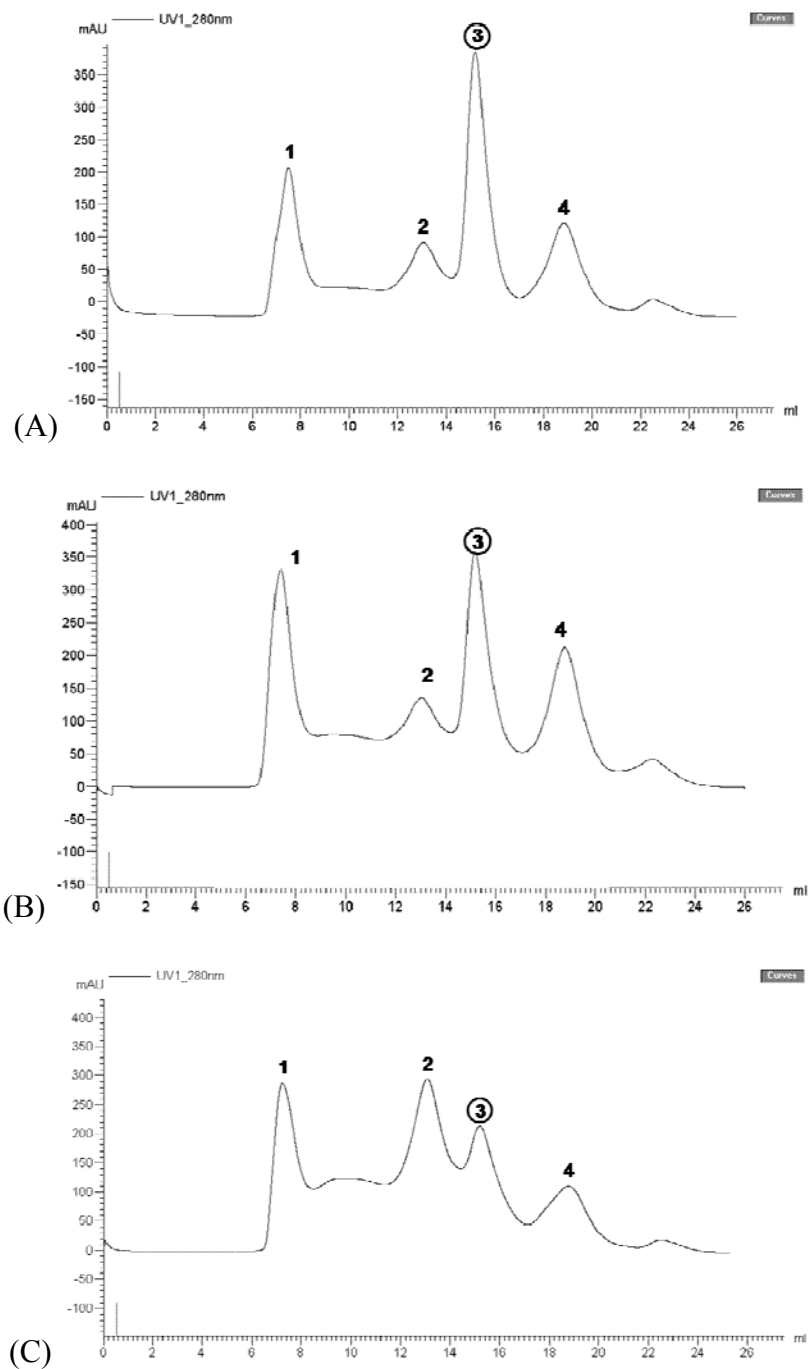


Figure 20: Chromatographic profile for the purification of activated Cyt2Aa2 (A), N89K (B) and T148K mutant (C). (number 1 to 4 are represented the peak's number. The circled number is the peak presenting toxin band.)

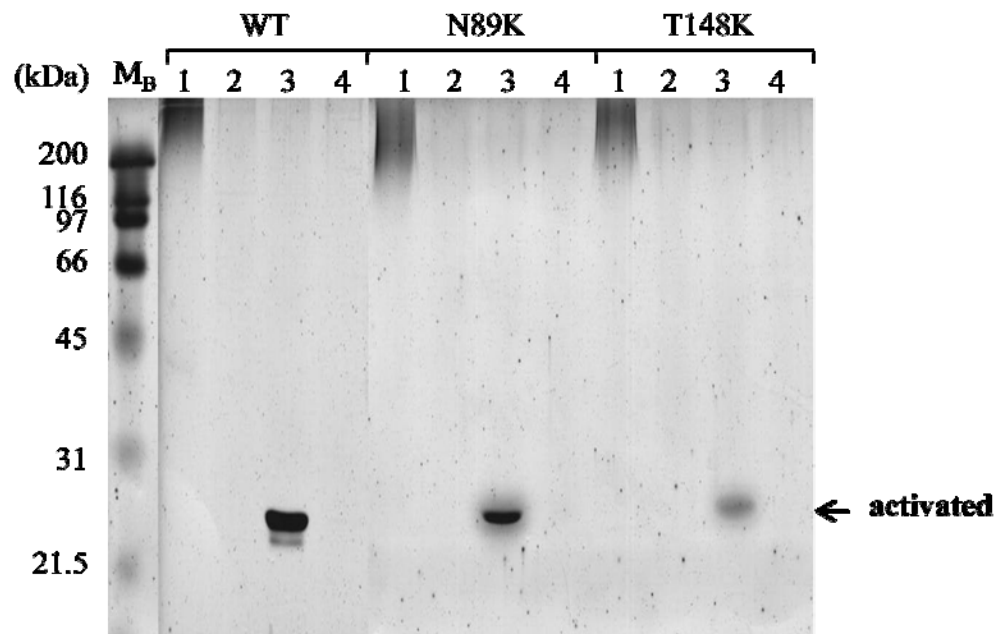


Figure 21: 12.5% SDS-PAGE of the elution fraction from size-exclusion chromatography

Lane M : broad-range protein marker

Lane 1-4 : purified toxin, peak 1 to peak 4

5.5 Intrinsic fluorescence spectroscopy

The 0.05 mg/ml purified protein sample was analyzed by intrinsic fluorescent spectrometry. The fluorescent spectra were scanned from 300 nm to 550 nm. The emission spectra gave two peaks for each sample, containing a major peak at about 330 nm and a minor is 340 nm (**figure 22**).

5.6 Trypsin digestion

After the proteinase K activated proteins were purified by Superdex 200™ column. The purified proteins were digested with trypsin (TPCK-treated) to check if the introduction of lysine residue could generate the cleavage site (**figure 23**). However, the result of silver staining and western blotting analysis did not show any difference of digestion pattern between the wild-type protein and the mutant protein. It was found that the trypsin-digested and non-digested products showed a molecular mass of 23 kDa.

5.7 Larvicidal activity

The larvicidal activity assay was performed by using the freshly prepared protoxins of Cyt2Aa2 wild-type, N89K and T148K for each individual experiments. The mortality of mosquitoes larvae after feeding with protoxin of wild-type, N89K or T148K was reported as the LC₅₀ value with their range after overnight incubation. The data was shown in **table 4**. The result showed that the toxicity against mosquitoes larvae of N89K and T148K mutant were somehow comparable to that of wild-type protoxin.

5.8 Hemolytic activity

A hemolytic activity was performed as a preliminary test for *in vitro* activity. The proteinase K activated protein, Cyt2Aa wild-type, N89K mutant, and T148K mutant, were incubated with sheep red blood cells for overnight. The results show that the wild-type and mutants could lyse the sheep RBCs (**figure 24**). While, the hemolytic activity of activated N89K was comparable to that of wild-type protein, the acitivity of T148K mutant was lower than that of the wild-type. The end point of

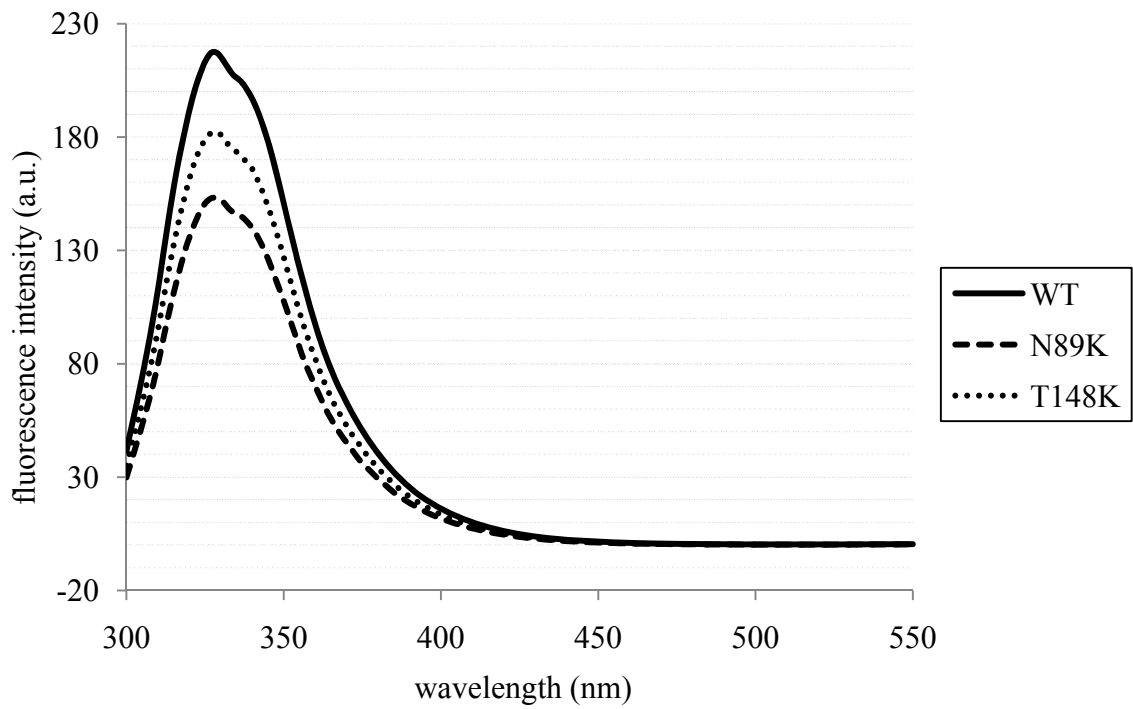


Figure 22: Intrinsic fluorescence spectra of the toxins.

The figure showed selective intrinsic fluorescence spectra of the activated toxin which was excited at 280 nm. The solid line represents wild type toxin. The dash line is N89K mutant and the dot line is T148K mutant.

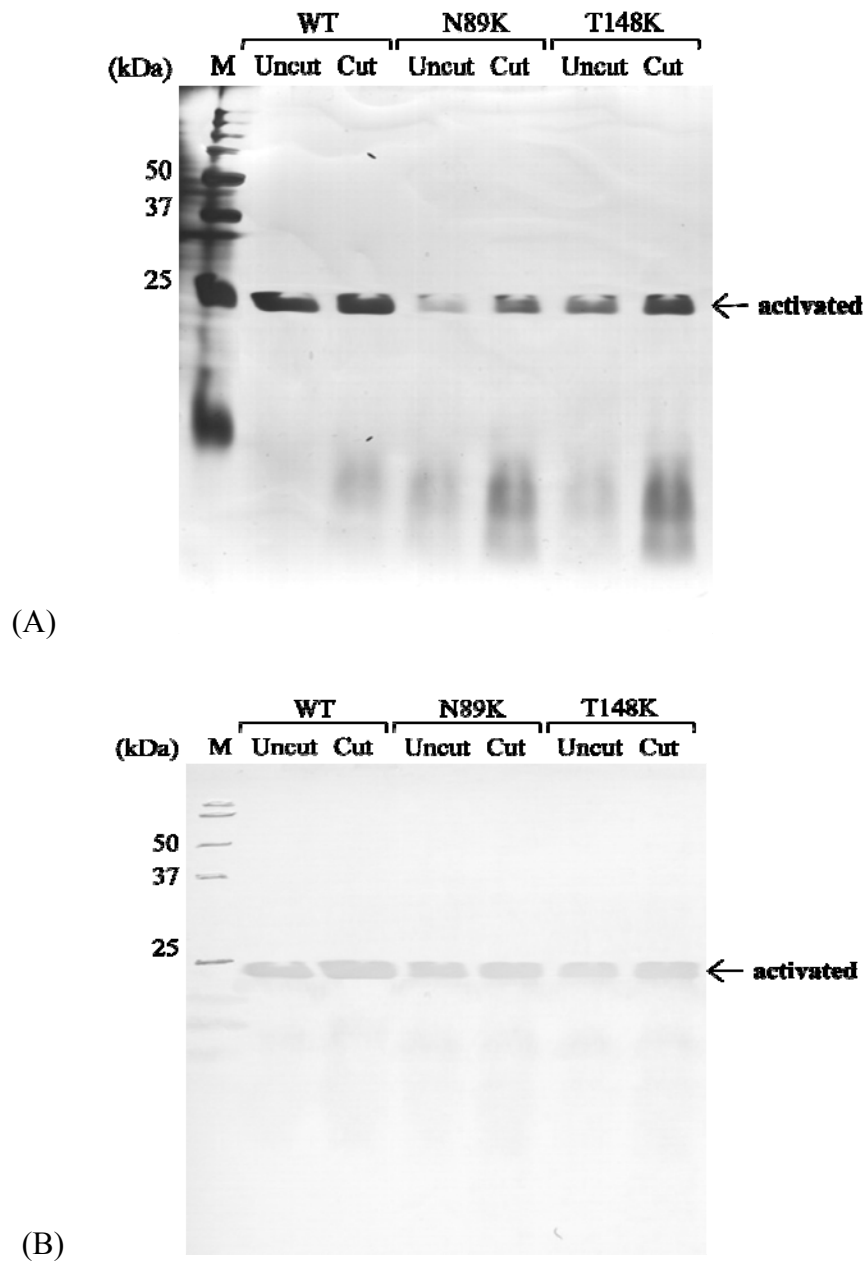
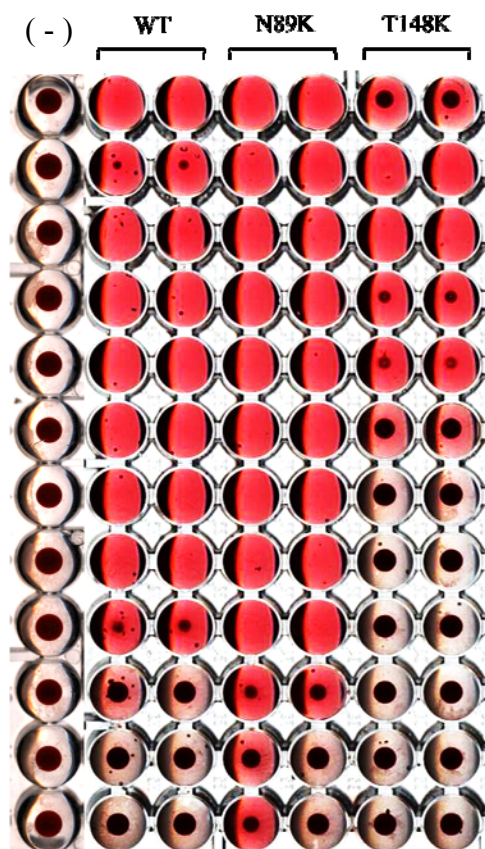


Figure 23: Trypsin digestion profile of N89K and T148K on the 15% SDS-PAGE gel (A) and Western blotting (B). (M: precision marker, Uncut: non-digested protein and Cut: digested product.)

| Exp. No. | LC ₅₀ (µg/ml) | | |
|----------------|---|---|---|
| | Wild-type | N89K | T148K |
| 1 | 0.044 (0.026 < LC ₅₀ < 0.057) | 0.049 (0.035 < LC ₅₀ < 0.059) | 0.037 (0.030 < LC ₅₀ < 0.044) |
| 2 | 0.044 (0.026 < LC ₅₀ < 0.057) | 0.025 (0.001 < LC ₅₀ < 0.037) | 0.139 (0.083 < LC ₅₀ < 0.234) |
| 3 | 0.044 (0.026 < LC ₅₀ < 0.057) | 0.041 (0.023 < LC ₅₀ < 0.055) | 0.069 (0.057 < LC ₅₀ < 0.082) |
| 4 | 0.057 (0.046 < LC ₅₀ < 0.071) | 0.125 (0.102 < LC ₅₀ < 0.153) | 0.043 (0.024 < LC ₅₀ < 0.078) |
| 5 | 0.020 (0.015 < LC ₅₀ < 0.025) | 0.020 (0.014 < LC ₅₀ < 0.026) | 0.098 (0.039 < LC ₅₀ < 0.246) |
| 6 | 0.067 (0.028 < LC ₅₀ < 0.159) | 0.079 (0.067 < LC ₅₀ < 0.093) | 0.099 (0.084 < LC ₅₀ < 0.115) |
| average | 0.046 ± 0.007 | 0.057 ± 0.016 | 0.081 ± 0.016 |

Table 4: The mosquitocidal activity of N89K and T148K mutant.

The 2-folds serial dilution of each toxin (wild type, N89K and T148K) was fed to 2-days old larvae for overnight at room temperature. The larval mortality was reported as means ± S.E.M. (S.E.M. = SD/√n, n=6).



| Toxin | Hemolytic end point (µg/ml) |
|---------|-----------------------------|
| Cyt2Aa2 | 0.059 |
| N89K | 0.151 |
| T148K | 0.516 |

Figure 24: Hemolytic activity.

All of samples were done as duplicate. The starting concentration of WT, N89K and T148K were 60, 133 and 33 µg/ml. Lane (-): PBS buffer as the negative control

Cyt2Aa2, N89K and T148K were 0.059 $\mu\text{g/ml}$, 0.151 $\mu\text{g/ml}$, and 0.516 $\mu\text{g/ml}$, respectively.

5.9 The hemoglobin release activity

The hemolytic activity of each toxin sample was reported as the percentage of RBCs lysis measured from the releasing of hemoglobin at 540 nm. The results, **figure 25**, showed that the hemolytic activity of N89K mutant is two –folds lower than that of the wild-type toxin. For the T148K mutant, the hemoglobin release activity was completely lost although dose of the protein was up to 4 $\mu\text{g/ml}$. This behavior was found similar for protein digested with proteinase K and chymotrypsin.

5.10 Oligomerization of the mutants

The 5 μg of the protein sample was incubated with the liposome and analyzed on SDS-PAGE gels. Both coomassie blue G and silver staining gels gave the same result showing that only N89K mutant toxin could oligomerise on the lipid membrane as same as the wild-type (The result showed the ladder pattern of the protein sample that incubated with liposome). T148K mutant could oligomerize in present of liposomes but not as good as wild type and N89K mutant (**figures 26 and 27**)

5.11 MTT cytotoxicity assay

The cytolytic activity of the mutants against mammalian cell lines (BHK(21)C13, IEC6 and HepG2) and mosquito cell line (C6/36) were reported as IC_{50} (**table 5**). The 50% lethal concentration of wild type against BHK(21)C13 is 0.56 $\mu\text{g/ml}$, against IEC6 is 5.83 $\mu\text{g/ml}$ and against HepG2 is 25.30 $\mu\text{g/ml}$. while T148K mutant is not cytolytic to the mammalian cell lines. The LC_{50} of wild type toxin against the C6/36 cell line is 1.93 $\mu\text{g/ml}$ while the LC_{50} of T148K is 21.00 $\mu\text{g/ml}$.

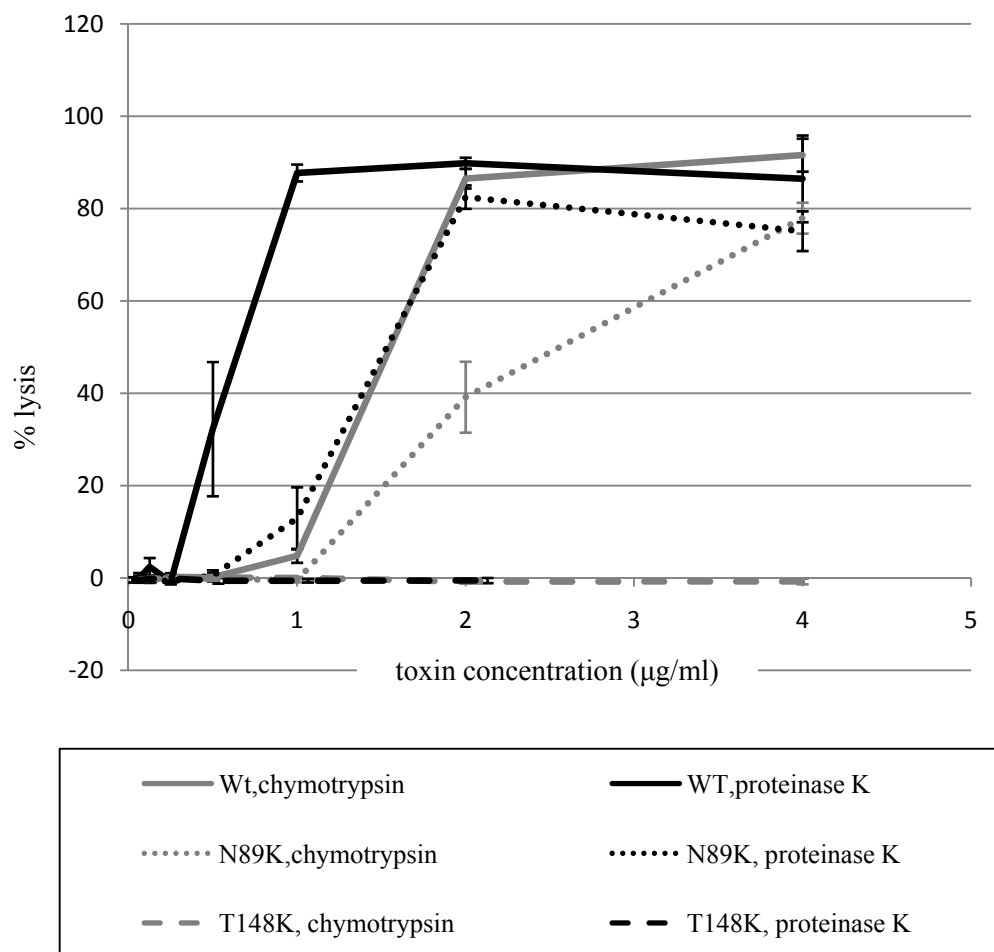


Figure 25: Hemoglobin release activity of Cyt2Aa2, N89K and T148K.

The activated Cyt2Aa2, N89K and T148K were mixed with 2% sheep red blood cells in PBS buffer for 1 hour at room temperature. The hemoglobin releasing was measured using the absorbance at 540 nm and reported as the means \pm S.E.M. (n=4). The gray lines represent the chymotrypsin-activated proteins while the black lines are the proteinase K-activated toxin. The solid, dot and dash line are wild type, N89K mutant and T148K mutant, respectively.

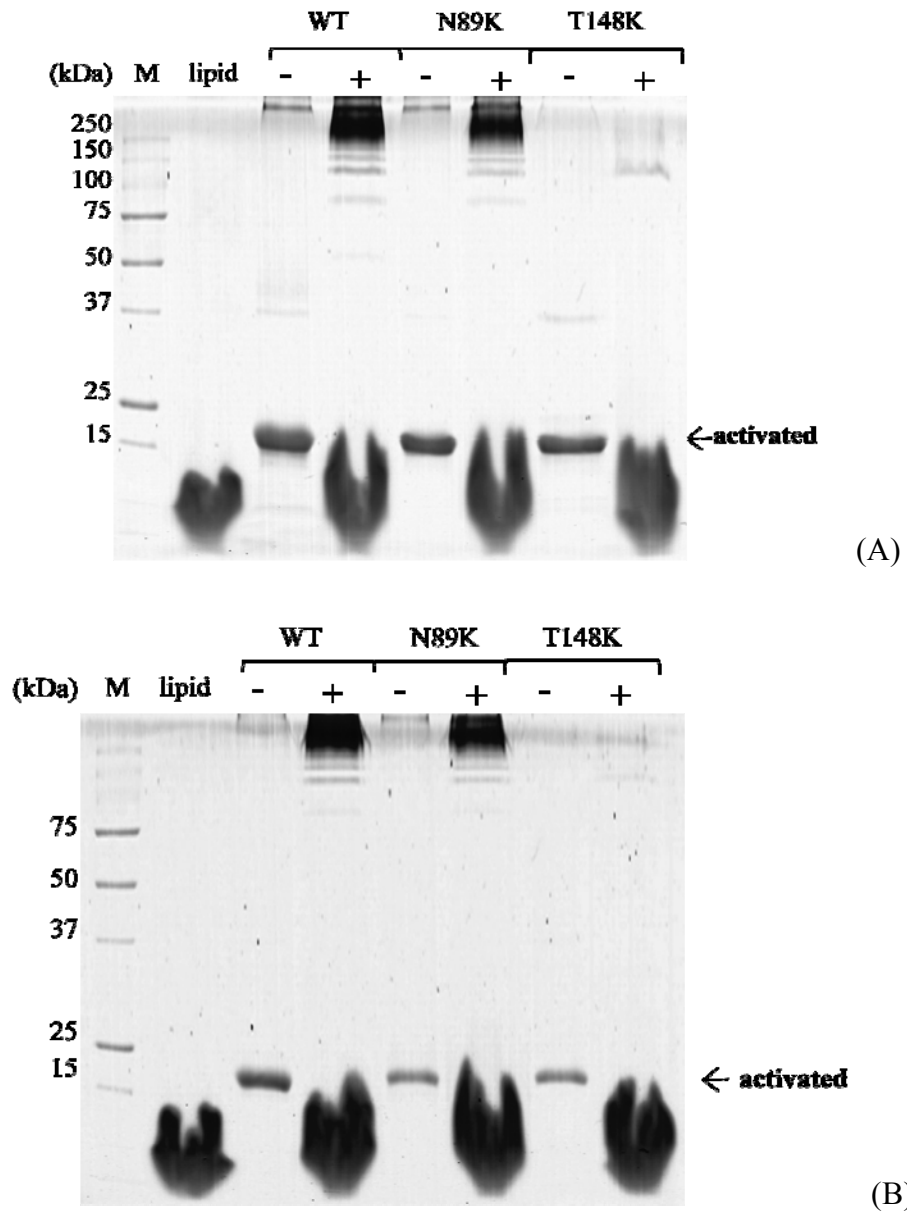


Figure 26: Oligomerization analysis with coomassie blue staining.

(A) proteinase K activated, (B) chymotrypsin activated.

M: precision protein marker

lipid: liposome only

- : activated toxins without liposome

+ : activated toxins with liposome

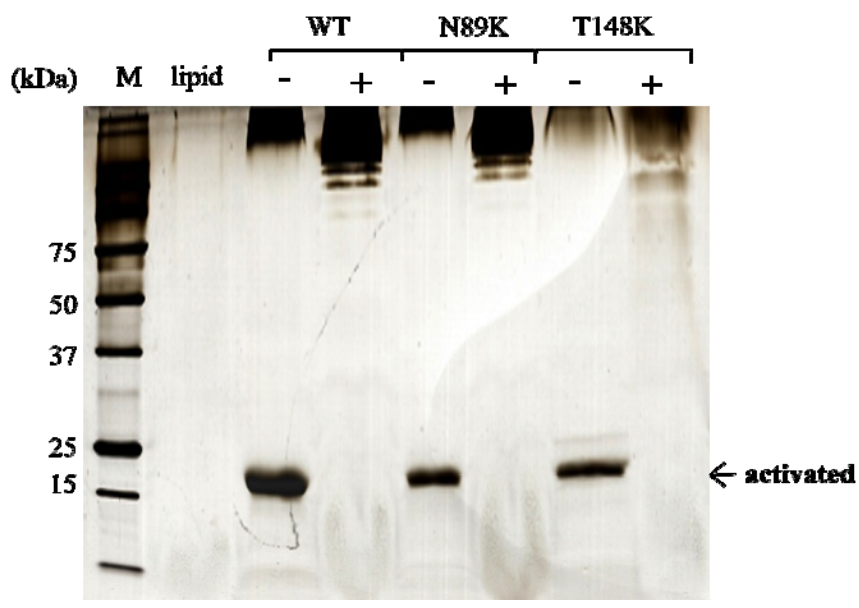
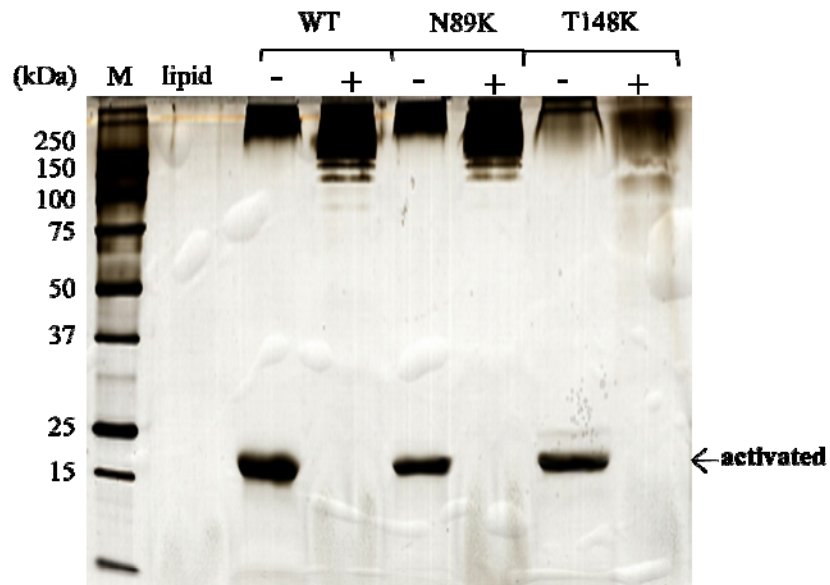


Figure 27: Oligomerization detected with silver staining.

(A) proteinase K activated, (B) chymotrypsin activated.

M: precision protein marker

lipid: liposome only

- : activated toxins without liposome

+ : activated toxins with liposome

Table 5: Cytotoxicity against four different cell lines (Sukitaya Veeranondha, MSc. Animal Cell Cytotoxicity Testing Service Bioassay Laboratory, BIOTEC)

1. BHK(21)C13 cell line

| Samples | %Survival at each concentration (ug/ml) compared to control | | | | | | | | IC ₅₀ (ug/ml) |
|---------|---|------|-----|------|------|-------|------|------|-----------------------------|
| | 60 | 30 | 15 | 7.5 | 3.75 | 1.875 | 0.93 | 0.46 | |
| 1 | 91 | 96 | 91 | 103 | 93 | 94 | 92 | 96 | - |
| 2 | 0 | 0.95 | 0 | 0.47 | 3 | 9 | 29 | 56 | 0.56 |
| 3 | 100 | 100 | 100 | 100 | 100 | 100 | 100 | 100 | - |

2. IEC6 cell line

| Samples | %Survival at each concentration (ug/ml) compared to control | | | | | | | | IC ₅₀ (ug/ml) |
|---------|---|------|------|-----|------|-------|------|------|-----------------------------|
| | 60 | 30 | 15 | 7.5 | 3.75 | 1.875 | 0.93 | 0.46 | |
| 1 | 85 | 87 | 86 | 86 | 88 | 88 | 94 | 98 | - |
| 2 | 0.29 | 0.88 | 6.76 | 29 | 78 | 86 | 88 | 90 | 5.83 |
| 3 | 96 | 94 | 85 | 88 | 84 | 90 | 89 | 86 | - |

3. HepG2 cell line

| Samples | %Survival at each concentration (ug/ml) compared to control | | | | | | | | IC ₅₀ (ug/ml) |
|---------|---|-----|-----|-----|------|-------|------|------|-----------------------------|
| | 60 | 30 | 15 | 7.5 | 3.75 | 1.875 | 0.93 | 0.46 | |
| 1 | 103 | 103 | 105 | 95 | 104 | 94 | 92 | 98 | - |
| 2 | 15 | 38 | 83 | 86 | 98 | 90 | 94 | 91 | 25.30 |
| 3 | 97 | 104 | 100 | 104 | 92 | 97 | 101 | 94 | - |

4. C6/36 cell line

| Samples | %Survival at each concentration (ug/ml) compared to control | | | | | | | | IC ₅₀ (ug/ml) |
|---------|---|------|------|-----|------|-------|------|------|-----------------------------|
| | 60 | 30 | 15 | 7.5 | 3.75 | 1.875 | 0.93 | 0.46 | |
| 1 | 97 | 90 | 104 | 102 | 100 | 100 | 100 | 100 | - |
| 2 | 0.08 | 0.61 | 1.15 | 0.8 | 13 | 53 | 88 | 102 | 1.93 |
| 3 | 18 | 44 | 58 | 94 | 100 | 100 | 100 | 100 | 21.00 |

The mean of each sample was equal to the mean of the control $\pm 10\%$ errors.

CHAPTER VI

DISCUSSION

The substitution of positively charged lysine in place of polar residue on the loop region between α B- β 3 and α D- β 4 has resulted in mutant toxins N89K and T148K, respectively. These mutants could be constructed by PCR-based site-directed mutagenesis. The PCR reactions were successfully performed at an annealing temperature of 45°C which is a low temperature for primers binding compared to the expected annealing temperature. In general the optimized temperature should not be lower than 5°C from the calculated melting temperature and should be between 50 -60°C. Lower annealing temperature can sometimes make the non-specific binding of the oligonucleotide primers to DNA template. However, the result from 1.2% agarose gel shows a strong band at 3.8 kb, considered to be the band of Cyt2Aa2. It means that the mutagenic primer sets can successfully bind to the expected site and produce the PCR product.

The obtained PCR products were confirmed for their nucleotide sequence by using restriction enzyme analysis and automated DNA sequencing. The results from restriction enzyme analysis gives the digestion profile of mutants different from the wild type plasmid as expected from prediction program. The result from automated nucleotide sequencing also confirms that the designed nucleotides substitution occurred at the expected site by mutagenesis and the rest of the whole sequence of Cyt2Aa2 gene is maintained.

The wild type and two mutant clones (N89K and T148K) were well expressed in the *Escherichia coli* system in the form of inclusion bodies. The cell culture of mutant T148K spends longer time than wild type and N89K to grow to an OD of 0.5 at 600 nm. This result suggests that *E. coli* cells containing T148K plasmids may produce product that toxic to the host cells, leading to deceleration of the cell growth and disturbing the protein expression. The inclusion toxins of wild type and mutants were isolated from the *E. coli* cells by French Pressure cell at 10,000 *psi*. In Carbonate

buffer pH 10.8, the solubility of N89K mutant was comparable to that of wild type, whereas the solubility of T148K was poorer than that of the wild type and N89K mutant. The results of toxin solubility assay revealed that the asparagines position 148 is important to solubilization of the toxin in carbonate buffer. On the other hands, the threonine position 89 may not play a crucial role in solubilization of the toxin protein. In the carbonate solubilization, both wild type and the mutants also showed some extra minor bands. There are two faint bands of molecular mass under 20 kDa and another band at molecular mass around 50 kDa. These extra-bands were then confirmed by using antibody against Cyt2Aa2 protein. The result from western blot analysis demonstrated that the two extra-bands of 15 kDa and 50 kDa are the products derived from Cyt2Aa2 protein. This 50 kDa protein fragment may represent the molecule of the protein dimer whilst the 15 kDa band may be the digested protein fragments by *E. coli* proteinase. A 15 kDa band was found as a very faint band on the SDS-PAGE gel. A threonine residue 148 may be a residue involving dimer formation. Lysine substitution at this site may disturb the interaction between monomers in the dimer molecules. While asparagines residue 89 may not involved with the dimer formation of this toxin. These protein samples were then divided into two groups, which were activated by 1% (v/v) proteinase K for 1 hour at 37°C and by 2% (v/v) chymotrypsin for 2 hours at 37°C. While the chymotrypsin activation did not decrease the amount of protein sample after digestion, the activation using proteinase K can significantly decreased the concentration of digested product about 5-folds lower than non-digested proteins. The difference in sensitivity of proteolysis of mutant proteins is possibly based on specificity of each protease. The chymotrypsin generally recognizes only the large hydrophatic residue such as tyrosine, tryptophan, and phenylalanine residue. The proteinase K has a broad specificity that cleaves the peptide bond nearby carboxyl group of aliphatic or aromatic amino acids (68). These results can provide a clue that the mutant T148K may be disrupted in its molecular stability as shown by the reduced expression, solubility and the digestion with proteinase K.

The purification of the proteinase K-activated proteins was accomplished by Superdex 200™ size-exclusion column. In the purification process, the proteins were monitored by measuring the UV absorption wavelength at 280 nm and reported as the chromatographic profile. The expected proteins were collected from eluted fractions

and confirmed by loading on the SDS-PAGE gel. From SDS-PAGE analysis, in the lane that are loaded with peak number 1 or void volume fraction we found some streak at the high molecular weight. It could be the result from self-aggregation of Cyt2Aa2 toxin. The purified proteins were then used for trypsin digestion. The digestion results of both wild type and mutants showed the same digestion pattern between non-digested and digested proteins (**figure 23**). Based on our analysis of toxin 3D structure by molecule visual program, the introduction of lysine in our mutants can interact with the adjacent amino acid. Lysine amino acid has a positive charge and a long side chain, consisting of four carbon atoms arrange inline and a NH_3 at the end of side-chain. The NH_3 residue in the long side chain of lysine may interact with the $-\text{OH}$ group of the neighboring amino acids. In N89K mutant the introducing lysine residue may bend down to interact with alanine residue 225 by *Van der Waals* force (**figure 28**). The lysine position 148 may possibly interact with the neighboring residue, aspartic acid residue 147 (**figure 29**). These interactions can block the side-chain of lysine from solvent exposure, leading to an unavailable tryptic site for trypsin.

The intrinsic fluorescent spectroscopy reveals the folding of mutant proteins by measurement the emission spectrum of protein that is excited by 280 nm ultra-violet light. The results of fluorescent spectra show that both of wild type and mutants give a similar major peak at wavelength of 328 nm. From this result, we can conclude that the substituted residue did not change the general folding of mutated proteins comparing to the wild type. The emission wavelength is based on the position and exposure of tryptophan residue on the protein. The tryptophan residue has the special properties that show a changing emission spectrum when surrounded with different microenvironment. From the emission spectra, the variation of the fluorescent intensity may occur from the unstable structure of the toxins or an error from toxin dilution.

The mechanism of Cyt2Aa2 toxin that specific β -sheets are inserted into the target cell membrane was proposed by B. Promdonkoy and D.J. Ellar (65). Their study focused on the pore formation of Cyt2Aa1 on the membrane of red blood cells. Initially, the toxin molecules attach the lipid membrane and insert β -sheet domain into membrane, as monomer, then the aggregation between each toxin molecule occur to

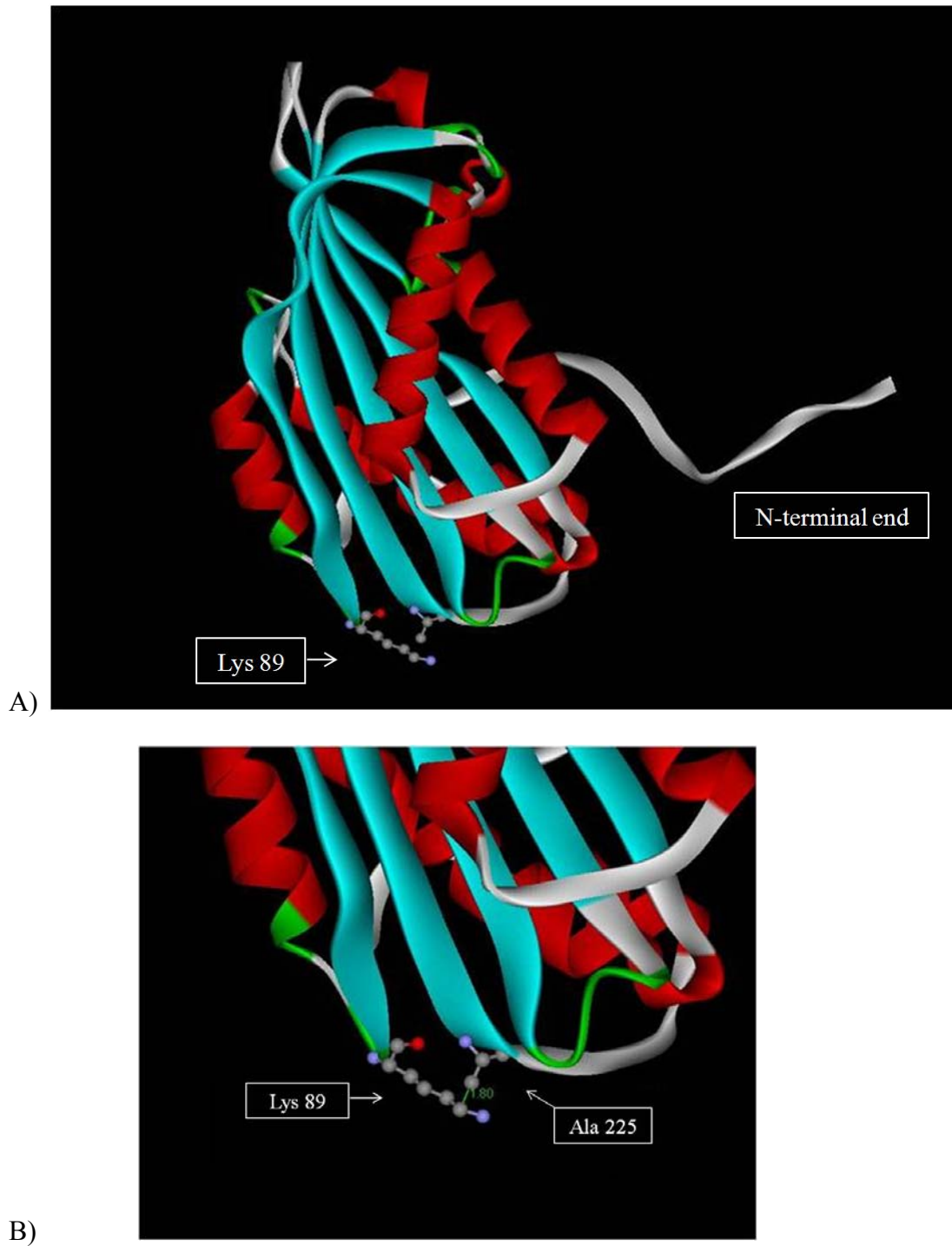


Figure 28: Possible conformation of lysine 89 that protect toxins from trypsin digestion.

Three-dimensional structure of Cyt2Aa2 toxin [A) and B)], constructed by WebLab viewer, shows the possible interaction between K89 and A225 by *Van der Waals* force.

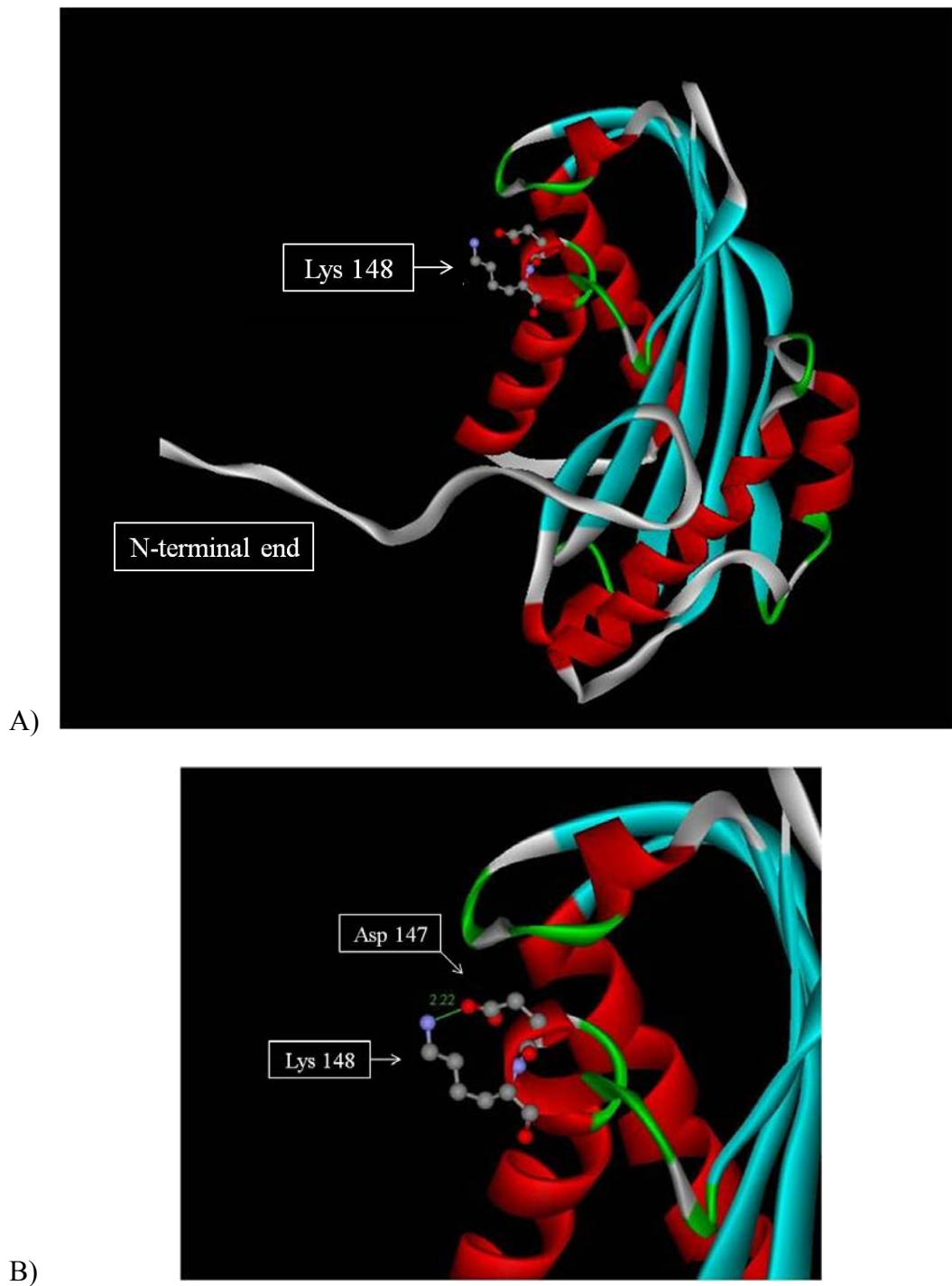


Figure 29: Possible interaction of lysine 148 on the Cyt2Aa2.

Three-dimensional structure [A) and B)], constructed by WebLab viewer, shows the possible interaction between lysine residue 148 and neighboring residue, aspartic acid 147 causing the reduction of solubilization and the protection from trypsin digestion.

form the β -barrel pore. In our study, the membrane recognition and oligomerization of the mutated proteins was analyzed by incubation with lipid vesicles. After incubation, the protein-lipid mixtures were collected by centrifugation at 12,000 rpm, and analyzed on 12.5% SDS-PAGE. From the polyacrylamine gel, the results of wild type and N89K samples obviously showed laddering pattern ranging from 75 kDa to molecular mass over 200 kDa, whereas the T148K mutant showed the very faint laddering pattern on the SDS-PAGE gel. These results suggest that the self-aggregation of mutant N89K and Cyt2Aa2 toxin could be found on the phosphatidylcholine liposome. However, the membrane recognition of T148K mutant may be lost when compared to that of the wild type toxin, suggesting that threonine residue 148 located on the loop between α -domain and β -domain may involve the recognition to phospholipid bilayers. On the opposite side of the toxin molecule, the lysine replacement at residue 89 does not disturb the conformation stability, specificity, and membrane recognition of the toxin. These results conclude that the asparagines residue 89 does not involve in membrane recognition and dimerization.

The biological activities of these mutants were analyzed both *in vivo* and *in vitro*. *In vivo* activity of the mutants was examined with 2 days old *A. aegypti* larvae which are reported as the susceptible strain of Cyt2Aa2 (60). For *in vitro* activity, the hemolytic activity assay and hemoglobin release assay were performed to analyze the cytolytic ability against sheep red blood cells.

The larvicidal activity assay was performed by adding the serial-dilutions of protein sample to *Aedes sp.* larvae. From the six separated larvicidal experiments, the results of the assay reveal that the Cyt2Aa2 protein is toxic to the larvae at LC₅₀ of 0.046 μ g/ml. In our assay, the larvicidal activity of 0.057 μ g/ml and 0.081 μ g/ml, are reported as the average 50% lethal concentration of N89K and T148K, respectively (Table 4). The lethal concentration of both mutants is comparable to that of the wild type protein. Recent paper that published by B. Promdonkoy, *et al.*, 2003 (69) reported the LC₅₀ of the Cyt2Aa2 toxin against *Aedes sp.* mosquitoes larvae at 0.5-1 μ g/ml. The larvicidal activity reported in this study seems to be better than that of the previously reported. This difference of susceptibility of the larvae may be due to the variation from age and size as the suggestion of Koni and Ellar, 1994 (32).

The end-points of hemolytic activity assay roughly show that the wild type protein is 0.059 µg/ml, while mutant N89K and T148K have the end-point at 0.151 µg/ml and 0.516 µg/ml, respectively. These results show that the hemolytic activity of mutant N89K is comparable to that of wild-type protein whereas T148K mutant has the end-point at the toxin concentration 10-folds higher than that of the wild-type proteins. The *in vitro* activity was confirmed by hemoglobin release assay using a serial dilution protein from 4 µg/ml to 0.03 µg/ml, incubated with 2% of sheep red blood cells. In case of proteinase K activation, the 50% of hemoglobin releasing was occurred at the concentration of 0.7 µg/ml for Cyt2Aa2 wild type, and 1.5 µg/ml for N89K mutant. On the other hand, the chymotrypsin activated proteins released hemoglobin at the concentration of 1.5 µg/ml and 2.5 µg/ml for Cyt2Aa2 and N89K mutant. Interestingly, the T148K cannot break the RBCs at the concentration of the activated protein is up to 4 µg/ml for proteinase K activation and 2 µg/ml for chymotrypsin activation. These results suggest that mutant T148K significantly reduces the hemolytic activity while mutant N89K still maintains the activity. It could be possible that a disruption is caused by the lysine residue, represent the positive charge, and affect the binding domain of the toxin.

Form the results of larvicidal activity and hemolytic activity assay, they show that the *in vivo* activity of the toxin can be different from *in vitro* activity, since there are many components and factors involving in the metabolism of living organism while *in vitro* activity was performed in control environment and minimal component.

In summary, the mutant N89K does not change any properties and biological activities from wild type toxin. The asparagine residue 89 should not be involved with the protein stabilization and function of Cyt2Aa2 toxin. The amino acid alignment also shows that the residue 89 is not a conserved amino acid between Cyt1A and Cyt2A (19). Moreover, it was proposed that asparagines 89 is rather involved with the β-sheet stabilization using hydrogen bonding interaction (19).

The results of T148K mutant show the decreasing of oligomerization of toxin on the lipid vesicle, *in vitro* that could be seen as a lack of laddering band (**figure 26 and 27**). It can be concluded that the threonine-148 residue may take part in membrane recognition of the toxin and the results of lysine substitution suggest that the polarity of the amino acid side chain may be important for membrane binding. In

addition, threonine 148 is a conserved residue between Cyt1A and Cyt2A toxin and expected to play role in the intermolecular interaction by *Van der Waals* bonding (19). The substituted lysine at residue 148 may cause the interruption of dimerization leading to unstable protein structure. Moreover, the introducing of lysine residue may disturb the protein stabilization by interaction of lysine 148 with aspartic acid residue 147, which proposed that plays role in dimerization activity of Cyt2Aa2 toxin (19). These interactions can cause the reduction of inclusion forming and protein solubilization in carbonate buffer, as shown in **figure 18**.

In general Cyt2Aa2 is toxic against *Aedes aegypti* larvae and sheep red blood cells, and also has a broad spectra to mammalian and mosquito cell line. In our experiment, the IC_{50} of the toxin against cell line of mosquito, human, rat and hamster are 1.93, 25.30, 5.83 and 0.56 $\mu\text{g/ml}$, respectively. Interestingly, the T148K mutant has a significant loss of the hemolytic activity and toxicity against human and animal cell lines *in vitro*. The reduction of broad cytolytic activity of Cyt2Aa2 toxin may be useful and help facilitate the scientists to develop the cytolytic toxin if high specificity to be used in the field of vector and pest control.

CHAPTER VII

SUMMARY

1. Tryptic digestion of N89K and T148K mutants was not detected because the substituted Lys may be not exposed to environment. The structural model suggests the interaction between Lys 89 and adjacent Ala 225, Lys 148 and the neighboring Asp 147.
2. Based on the native-liked structure and biological activities, *in vivo* and *in vitro*, of N89K, it is suggested that Asn 89 may not be a crucial residue involved in the structural stabilization and biological function.
3. The results of *in vitro* assay revealed that lysine substitution at Thr-148 affects hemolytic activity and toxin oligomerization in liposome. However structural analysis of the mutant toxin shows a similar folding to that of wild type.
4. From *in vitro* cytotoxicity assay, T148K has lost its cytolytic activity to mammalian cell lines. However T148K have a slight cytolyticity against *Aedes abopictus* cell line.
5. Thr-148 may possibly plays role in the membrane recognition and binding of the Cyt2Aa2 toxin.
6. A reduction of broad range cytolytic activity of T148K mutant may help improve the non-specific activity of cytolytic toxin for the future use in medical treatment and vector control.

REFERENCES

1. Nickerson KW, De Pinto J, Bulla LA, Jr. Lipid metabolism during bacterial growth, sporulation, and germination: kinetics of fatty acid and macromolecular synthesis during spore germination and outgrowth of *Bacillus thuringiensis*. *J Bacteriol.* 1975 Jan;121(1):227-33.
2. Schesser JH, Bulla LA, Jr. Toxicity of *Bacillus thuringiensis* spores to the tobacco hornworm, *Manduca sexta*. *Appl Environ Microbiol.* 1978 Jan;35(1):121-3.
3. Somerville HJ, Pockett HV. An insect toxin from spores of *Bacillus thuringiensis* and *Bacillus cereus*. *J Gen Microbiol.* 1975 Apr;87(2):359-69.
4. Ulewicz K. Studies of the infection of the cockroaches (*Blattella germanica*[L.]) with *Bac. thuringiensis*. *Zentralbl Bakteriol [Orig B].* 1975 Jul;160(4-5):534-9.
5. Vervelle C. The role of spores and crystals of *Bacillus thuringiensis* Berliner in the infection of *Laspeyresia pomonella* L. (Tortricidae) (author's transl). *Ann Parasitol Hum Comp.* 1975 Nov-Dec;50(6):655-68.
6. Schnepf E, Crickmore N, Van Rie J, Lereclus D, Baum J, Feitelson J, et al. *Bacillus thuringiensis* and its pesticidal crystal proteins. *Microbiol Mol Biol Rev.* 1998 Sep;62(3):775-806.
7. Lacey LA, Escaffre H, Philippon B, Seketeli A, Guillet P. Large river treatment with *Bacillus thuringiensis* (H-14) for the control of *Simulium damnosum* s.l. in the Onchocerciasis Control Programme. *Tropenmed Parasitol.* 1982 Jun;33(2):97-101.
8. Mulla MS, Federici BA, Darwazeh HA, Ede L. Field evaluation of the microbial insecticide *Bacillus thuringiensis* serotype H-14 against floodwater mosquitoes. *Appl Environ Microbiol.* 1982 Jun;43(6):1288-93.
9. Rampal L, Thevasagayam ES, Kolta S, Cheong WH. A small scale field trial with *Bacillus thuringiensis* against culicine mosquitoes, Kelang, Malaysia. *Southeast Asian J Trop Med Public Health.* 1983 Mar;14(1):101-5.

10. Schesser JH. Commercial formulations of *Bacillus thuringiensis* for control of Indian meal moth. *Appl Environ Microbiol.* 1976 Oct;32(4):508-10.
11. Calabrese DM, Nickerson KW, Lane LC. A comparison of protein crystal subunit sizes in *Bacillus thuringiensis*. *Can J Microbiol.* 1980 Aug;26(8):1006-10.
12. Schnepf HE, Wong HC, Whiteley HR. The amino acid sequence of a crystal protein from *Bacillus thuringiensis* deduced from the DNA base sequence. *J Biol Chem.* 1985 May 25;260(10):6264-72.
13. Tyrell DJ, Bulla LA, Jr., Andrews RE, Jr., Kramer KJ, Davidson LI, Nordin P. Comparative biochemistry of entomocidal parasporal crystals of selected *Bacillus thuringiensis* strains. *J Bacteriol.* 1981 Feb;145(2):1052-62.
14. Andrews RE, Jr., Bibilos MM, Bulla LA, Jr. Protease activation of the entomocidal protoxin of *Bacillus thuringiensis* subsp. *kurstaki*. *Appl Environ Microbiol.* 1985 Oct;50(4):737-42.
15. Armstrong JL, Rohrmann GF, Beaudreau GS. Delta endotoxin of *Bacillus thuringiensis* subsp. *israelensis*. *J Bacteriol.* 1985 Jan;161(1):39-46.
16. Bulla LA, Jr., Kramer KJ, Davidson LI. Characterization of the entomocidal parasporal crystal of *Bacillus thuringiensis*. *J Bacteriol.* 1977 Apr;130(1):375-83.
17. Hofte H, Whiteley HR. Insecticidal crystal proteins of *Bacillus thuringiensis*. *Microbiol Rev.* 1989 Jun;53(2):242-55.
18. Aronson AI, Beckman W, Dunn P. *Bacillus thuringiensis* and related insect pathogens. *Microbiol Rev.* 1986 Mar;50(1):1-24.
19. Li J, Koni PA, Ellar DJ. Structure of the mosquitocidal delta-endotoxin CytB from *Bacillus thuringiensis* sp. *kyushuensis* and implications for membrane pore formation. *J Mol Biol.* 1996 Mar 22;257(1):129-52.
20. Koni PA, Ellar DJ. Cloning and characterization of a novel *Bacillus thuringiensis* cytolytic delta-endotoxin. *J Mol Biol.* 1993 Jan 20;229(2):319-27.
21. Thomas WE, Ellar DJ. Mechanism of action of *Bacillus thuringiensis* var *israelensis* insecticidal delta-endotoxin. *FEBS Lett.* 1983 Apr 18;154(2):362-8.
22. Gill SS, Hornung JM. Cytolytic activity of *Bacillus thuringiensis* proteins to insect and mammalian cell lines. *J Invertebr Pathol.* 1987 Jul;50(1):16-25.

23. Waalwijk C, Dullemans AM, van Workum ME, Visser B. Molecular cloning and the nucleotide sequence of the Mr 28 000 crystal protein gene of *Bacillus thuringiensis* subsp. *israelensis*. *Nucleic Acids Res.* 1985 Nov 25;13(22):8207-17.
24. Ward ES, Ellar DJ. *Bacillus thuringiensis* var. *israelensis* delta-endotoxin. Nucleotide sequence and characterization of the transcripts in *Bacillus thuringiensis* and *Escherichia coli*. *J Mol Biol.* 1986 Sep 5;191(1):1-11.
25. Ward ES, Ellar DJ, Todd JA. Cloning and expression in *Escherichia coli* of the insecticidal delta-endotoxin gene of *Bacillus thuringiensis* var. *israelensis*. *FEBS Lett.* 1984 Oct 1;175(2):377-82.
26. Crickmore N, Zeigler DR, Feitelson J, Schnepf E, Van Rie J, Lereclus D, et al. Revision of the nomenclature for the *Bacillus thuringiensis* pesticidal crystal proteins. *Microbiol Mol Biol Rev.* 1998 Sep;62(3):807-13.
27. Guerchicoff A, Delecluse A, Rubinstein CP. The *Bacillus thuringiensis* cyt genes for hemolytic endotoxins constitute a gene family. *Appl Environ Microbiol.* 2001 Mar;67(3):1090-6.
28. Bourgouin C, Klier A, Rapoport G. Characterization of the genes encoding the haemolytic toxin and the mosquitocidal delta-endotoxin of *Bacillus thuringiensis israelensis*. *Mol Gen Genet.* 1986 Dec;205(3):390-7.
29. Adams LF, Visick JE, Whiteley HR. A 20-kilodalton protein is required for efficient production of the *Bacillus thuringiensis* subsp. *israelensis* 27-kilodalton crystal protein in *Escherichia coli*. *J Bacteriol.* 1989 Jan;171(1):521-30.
30. McLean KM, Whiteley HR. Expression in *Escherichia coli* of a cloned crystal protein gene of *Bacillus thuringiensis* subsp. *israelensis*. *J Bacteriol.* 1987 Mar;169(3):1017-23.
31. Visick JE, Whiteley HR. Effect of a 20-kilodalton protein from *Bacillus thuringiensis* subsp. *israelensis* on production of the CytA protein by *Escherichia coli*. *J Bacteriol.* 1991 Mar;173(5):1748-56.
32. Koni PA, Ellar DJ. Biochemical characterization of *Bacillus thuringiensis* cytolytic delta-endotoxins. *Microbiology.* 1994 Aug;140 (Pt 8):1869-80.

33. Tepanant W. Investigation of folding pathway of Cyt2Aa2 Insecticidal Protein from *Bacillus thuringiensis*. Nakron Pathom: MAHIDOL University; 2004.
34. Earp DJ, Ellar DJ. *Bacillus thuringiensis* var. *morrisoni* strain PG14: nucleotide sequence of a gene encoding a 27kDa crystal protein. *Nucleic Acids Res.* 1987 Apr 24;15(8):3619.
35. Galjart NJ, Sivasubramanian N, Federici BA. Plasmid location, cloning, and sequence analysis of the gene encoding a 27.3-kilodalton cytolytic protein from *Bacillus thuringiensis* subsp. *morrisoni* (PG-14). *Current Microbiology.* 1987;16(3):171-7.
36. Thiery I, Delecluse A, Tamayo MC, Orduz S. Identification of a gene for Cyt1A-like hemolysin from *Bacillus thuringiensis* subsp. *medellin* and expression in a crystal-negative *B. thuringiensis* strain. *Appl Environ Microbiol.* 1997 February 1, 1997;63(2):468-73.
37. Payne JD, CA), Narva, Kenneth E. (San Diego, CA), Uyeda, Kendrick A. (San Diego, CA), Stalder, Christine J. (San Diego, CA), Michaels, Tracy E. (Ames, IA), inventor Mycogen Corporation (San Diego, CA), assignee. *Bacillus thuringiensis* isolate PS201T6 toxin. United States. 1995.
38. Promdonkoy B, Chewawiwat N, Tanapongpipat S, Luxananil P, Panyim S. Cloning and Characterization of a Cytolytic and Mosquito Larvicidal δ -Endotoxin from *Bacillus thuringiensis* subsp. *darmstadiensis*. *Current Microbiology.* 2003;46(2):0094-8.
39. Guerchicoff A, Ugalde RA, Rubinstein CP. Identification and characterization of a previously undescribed cyt gene in *Bacillus thuringiensis* subsp. *israelensis*. *Appl Environ Microbiol.* 1997 July 1, 1997;63(7):2716-21.
40. Yu J, Xu W, Zeng S, Zhang X, Liu J, Xie R, et al. Cloning and expression of cyt2Ba7 gene from a soil-isolated *Bacillus thuringiensis*. *Curr Microbiol.* 2002 Mar;45(5):309-14.
41. Cheong H, Gill SS. Cloning and characterization of a cytolytic and mosquitocidal delta-endotoxin from *Bacillus thuringiensis* subsp. *jegathesan*. *Appl Environ Microbiol.* 1997 Aug;63(8):3254-60.

42. Juarez-Perez V, Guerchicoff A, Rubinstein C, Delecluse A. Characterization of Cyt2Bc Toxin from *Bacillus thuringiensis* subsp. *medellin*. *Appl Environ Microbiol.* 2002 March 1, 2002;68(3):1228-31.
43. Butko P. Cytolytic toxin Cyt1A and its mechanism of membrane damage: data and hypotheses. *Appl Environ Microbiol.* 2003 May;69(5):2415-22.
44. Manceva SD, Pusztai-Carey M, Russo PS, Butko P. A detergent-like mechanism of action of the cytolytic toxin Cyt1A from *Bacillus thuringiensis* var. *israelensis*. *Biochemistry.* 2005 Jan 18;44(2):589-97.
45. Knowles BH, Blatt MR, Tester M, Horsnell JM, Carroll J, Menestrina G, et al. A cytolytic delta-endotoxin from *Bacillus thuringiensis* var. *israelensis* forms cation-selective channels in planar lipid bilayers. *FEBS Lett.* 1989 Feb 27;244(2):259-62.
46. Szabo E, Murvai J, Fabian P, Fabian F, Hollosi M, Kajtar J, et al. Is an amphiphilic region responsible for the haemolytic activity of *Bacillus thuringiensis* toxin? *Int J Pept Protein Res.* 1993 Dec;42(6):527-32.
47. Gazit E, Shai Y. Structural characterization, membrane interaction, and specific assembly within phospholipid membranes of hydrophobic segments from *Bacillus thuringiensis* var. *israelensis* cytolytic toxin. *Biochemistry.* 1993 Nov 23;32(46):12363-71.
48. Jap BK, Walian PJ. Biophysics of the structure and function of porins. *Q Rev Biophys.* 1990 Nov;23(4):367-403.
49. Moniatte M, van der Goot FG, Buckley JT, Pattus F, van Dorselaer A. Characterisation of the heptameric pore-forming complex of the *Aeromonas* toxin aerolysin using MALDI-TOF mass spectrometry. *FEBS Lett.* 1996 Apr 22;384(3):269-72.
50. Promdonkoy B, Ellar DJ. Membrane pore architecture of a cytolytic toxin from *Bacillus thuringiensis*. *Biochem J.* 2000 Aug 15;350 Pt 1:275-82.
51. Knowles BHE, D. J. Colloid-osmotic lysis is a general feature of the mechanism of action of *Bacillus thuringiensis* δ -endotoxins with different insect specificity. *Biochim Biophys Acta.* 1987;924:509-18.

52. Perlak FJ, Stone TB, Muskopf YM, Petersen LJ, Parker GB, McPherson SA, et al. Genetically improved potatoes: protection from damage by Colorado potato beetles. *Plant Mol Biol.* 1993 May;22(2):313-21.
53. Perlak FJ, Fuchs RL, Dean DA, McPherson SL, Fischhoff DA. Modification of the coding sequence enhances plant expression of insect control protein genes. *Proc Natl Acad Sci U S A.* 1991 Apr 15;88(8):3324-8.
54. Lynch RE, Wiseman BR, Plaisted D, Warnick D. Evaluation of transgenic sweet corn hybrids expressing CryIA (b) toxin for resistance to corn earworm and fall armyworm (Lepidoptera: Noctuidae). *J Econ Entomol.* 1999 Feb;92(1):246-52.
55. Bravo A, Gill SS, Soberon M. Mode of action of *Bacillus thuringiensis* Cry and Cyt toxins and their potential for insect control. *Toxicon.* 2007 Mar 15;49(4):423-35.
56. Wirth MC, Walton WE, Federici BA. Cyt1A from *Bacillus thuringiensis* Restores Toxicity of *Bacillus sphaericus* Against Resistant *Culex quinquefasciatus* (Diptera: Culicidae). *Journal of Medical Entomology.* 2000 May 01, 2000;37(3):401-7.
57. Neil Crickmore EBJAWDJJE. Contribution of the individual components of the δ -endotoxin crystal to the mosquitocidal activity of *Bacillus thuringiensis* subsp. *israelensis*. *FEMS Microbiology Letters.* 1995;131(3):249-54.
58. Abdullah MA, Alzate O, Mohammad M, McNall RJ, Adang MJ, Dean DH. Introduction of *Culex* toxicity into *Bacillus thuringiensis* Cry4Ba by protein engineering. *Appl Environ Microbiol.* 2003 Sep;69(9):5343-53.
59. Al-yahyaee SAS, Ellar DJ. Cell Targeting of a Pore-Forming Toxin, CytA δ-Endotoxin from *Bacillus thuringiensis* Subspecies *israelensis*, by Conjugating CytA with Anti-Thy 1 Monoclonal Antibodies and Insulin. *Bioconjugate Chem.* 1996;7(4):451-60.
60. Promdonkoy B, Chewawiwat N, Tanapongpipat S, Luxananil P, Panyim S. Cloning and characterization of a cytolytic and mosquito larvicidal delta-endotoxin from *Bacillus thuringiensis* subsp. *darmstadiensis*. *Curr Microbiol.* 2003 Feb;46(2):94-8.

61. Joseph Sambrook DR. *Molecular Cloning; A Molecular Biology; Laboratory Manuals/Handbooks* third edition ed. Cold Spring Harbor, New York: Cold Spring Harbor Laboratory; 2001.
62. Bimboim HC, Doly J. A rapid alkaline extraction procedure for screening recombinant plasmid DNA. *Nucl Acids Res.* 1979 November 24, 1979;7(6):1513-23.
63. Bradford MM. A rapid and sensitive method for the quantitation of microgram quantities of protein utilizing the principle of protein-dye binding. *Anal Biochem.* 1976 May 7;72:248-54.
64. Vanderheiden GJ, Fairchild AC, Jago GR. Construction of a laboratory press for use with the French pressure cell. *Appl Microbiol.* 1970 May;19(5):875-7.
65. Promdonkoy B, Ellar DJ. Investigation of the pore-forming mechanism of a cytolytic delta-endotoxin from *Bacillus thuringiensis*. *Biochem J.* 2003 Aug 15;374(Pt 1):255-9.
66. Waddell WJ. A simple ultraviolet spectrophotometric method for the determination of protein. *J Lab Clin Med.* 1956 Aug;48(2):311-4.
67. Mosmann T. Rapid colorimetric assay for cellular growth and survival: application to proliferation and cytotoxicity assays. *J Immunol Methods.* 1983 Dec 16;65(1-2):55-63.
68. Wolfgang Ebeling NHMKHMHDOHL. Proteinase K from *Tritirachium album* Limber. *European Journal of Biochemistry.* 1974;47(1):91-7.
69. Promdonkoy B, Ellar DJ, Chewawiwat N, Tanapongpipat S, Luxananil P, Panyim S. Investigation of the pore-forming mechanism of a cytolytic delta-endotoxin from *Bacillus thuringiensis*. *Biochem J.* 2003 Aug 15;374(Pt 1):255-9.

BIOGRAPHY

| | |
|------------------------------|--|
| NAME | Mr. Boonsan Prasertkulchai |
| DATE OF BIRTH | January 7, 1983 |
| PLACE OF BIRTH | Bangkok, Thailand |
| INSTITUTIONS ATTENDED | Mahidol University, 2001-2004: Bachelor of Science (Biology) Mahidol University, 2005-2008: Master of Science (Molecular Genetics and Genetic Engineering) |
| HOME ADDRESS | 79 Charansanitwong 46, Bangyi Kan, Bangplad, Bangkok 10700. Tel. 02-4347811 E-mail: ann_the_little@yahoo.com |